THE JOURNAL OF BIOLOGICAL CHEMISTRY VOL. 290, NO. 15, pp. 9626–9645, April 10, 2015

Protein Kinase A (PknA) of *Mycobacterium tuberculosis* Is Independently Activated and Is Critical for Growth *in Vitro* and Survival of the Pathogen in the Host*

Received for publication, September 13, 2014, and in revised form, February 10, 2015 Published, JBC Papers in Press, February 20, 2015, DOI 10.1074/jbc.M114.611822

Sathya Narayanan Nagarajan[‡§], Sandeep Upadhyay[‡], Yogesh Chawla[‡1], Shazia Khan[‡2], Saba Naz[‡], Jayashree Subramanian[§], Sheetal Gandotra[¶], and Vinay Kumar Nandicoori[‡3]

From the [‡]National Institute of Immunology, Aruna Asaf Ali Marg, New Delhi 110067, India, the [§]Department of Biotechnology, Nehru Arts and Science College, Coimbatore 641105, India, and [¶]CSIR-Institute of Genomics and Integrative Biology, Mathura Road, New Delhi 110020, India

Background: Protein kinase A has been shown to be involved in modulating critical functions.
Results: Although the activity of PknA is crucial for cell growth, the extracellular domain is expendable.
Conclusion: Although the activation of PknA is necessary for its function, this is independent of PknB.
Significance: PknA plays an indispensable role and is required for both *in vitro* and *in vivo* growth.

The essential mycobacterial protein kinases PknA and PknB play crucial roles in modulating cell shape and division. However, the precise *in vivo* functional aspects of PknA have not been investigated. This study aims to dissect the role of PknA in mediating cell survival *in vitro* as well as *in vivo*. We observed aberrant cell shape and severe growth defects when PknA was depleted. Using the mouse infection model, we observe that PknA is essential for survival of the pathogen in the host. Complementation studies affirm the importance of the kinase, juxtamembrane, and transmembrane domains of PknA. Surprisingly, the extracytoplasmic domain is dispensable for cell growth and survival *in vitro*. We find that phosphorylation of the activation loop at Thr^{172} of PknA is critical for bacterial growth. PknB has been previously suggested to be the receptor kinase, which activates multiple kinases, including PknA, by trans-phosphorylating their activation loop residues. Using phospho-specific PknA antibodies and conditional *pknB* mutant, we find that PknA autophosphorylates its activation loop independent of PknB. Fluorescently tagged PknA and PknB show distinctive distribution patterns within the cell, suggesting that although both kinases are known to modulate cell shape and division, their modes of action are likely to be different. This is supported by our findings that expression of kinase-dead PknA *versus* kinase-dead PknB in mycobacterial cells leads to different cellular phenotypes. Data indicate that although PknA and PknB are expressed as part of the same operon, they appear to be regulating cellular processes through divergent signaling pathways.

The response to environmental change is often manifested through post-translational modifications of the proteome, such as phosphorylation (1), acetylation (2), and ubiquitination (3), among others. Protein phosphorylation events are especially known for their influence on the regulation of a number of cellular processes, including gene regulation (4, 5), cell growth, and division (6). Although Ser/Thr/tyrosine kinases are widely prevalent in higher eukaryotes (7, 8), in bacterial systems, cellular processes are largely modulated by two-component signaling cascades and bacterial tyrosine kinases (BY kinases) (9, 10). Phosphorylation's mediated through BY kinases have been shown to regulate a wide array of physiological process among bacteria that includes DNA replication, virulence, and antibiotic resistance (11–13). PtkA, a mycobacterial tyrosine kinase, has tyrosine phosphorylation activity and was shown to phosphorylate its cognate phosphatase PtpA (14). The analyses of the whole genome sequences of several pathogens, including mycobacterial species, *Yersinia*, *Streptococcus* etc., however, has revealed the presence of Ser/Thr protein kinases in them (15–18).

PknA and PknB are known to have profound effects on processes involved in determining cell shape and morphology and possibly cell division. Kang *et al.* (19) have demonstrated that subtle differences in expression levels of PknA or PknB have deleterious effects on mycobacteria. PknA has been shown to regulate morphological changes associated with cell division, and its overexpression gives rise to elongated and branched structures (19, 20). PknB overexpression has been reported to result in widened and bulging cells. Overexpression in both cases led to decreased growth rate of the bacilli (19). PknA and PknB consist of an ~270-aa[4] intracellular kinase domain, an ~60–70-aa juxtamembrane domain, and an ~20-aa transmembrane domain connected to an extracellular domain. Although the extracellular region of PknA is relatively short

* This work was supported by Department of Biotechnology, Government of India, Grant BT/PR5557/Med/29/526/2012 (to V. K. N.) and Council of Scientific and Industrial Research, Grant BSC0403 (to S. G.).
[1] Senior Research Fellow of the Council of Scientific and Industrial Research.
[2] Present address: Wellman Center for Photomedicine, Massachusetts General Hospital, Harvard Medical School, Boston, MA 02114.
[3] To whom correspondence should be addressed. Tel.: 91-11-26703789; Fax: 91-11-26742125; E-mail: vinaykn@nii.ac.in.

[4] The abbreviations used are: aa, amino acid(s); PASTA, protein and serine/threonine kinase-associated; ATc, anhydrotetracycline; IVN, isovaleronitrile; WCL, whole cell lysate; pptr, pristinamycin-inducible promoter; TM, transmembrane motif; KD, kinase domain; JM, juxtamembrane domain; TATA, T172A,T174A double mutant; T3A, T172A,T174A,T180A triple mutant; Van-FL, vancomycin-fluorescein; STPK, Ser/Thr protein kinase; MBP, maltose-binding protein; p-PknA, PknA-Thr(P)^{172},Thr(P)^{174}.

TABLE 1
Strains used in the study

Strains	Description	Source
DH5α	*E. coli* strain used for cloning experiments	Invitrogen
BL21 (DE3) codon plus	*E. coli* strain used for protein expression	Stratagene
mc^2155	Wild type *M. smegmatis* strain	ATCC, 700084
mc^2155::HiA-PknA	mc^2155 strain electroporated with integrative proficient pST-HiA-PknA wherein *pknA* expression is under the regulation of inducible acetamidase promoter; Hyg^r	This study
$mc^2\Delta pknA$	*M. smegmatis pknA* conditional gene replacement mutant; Hyg^r	This study
$mc^2\Delta pknA$::pNit	$mc^2\Delta pknA$ electroporated with pNit vector (33); Hyg^r, Kan^r	This study
$mc^2\Delta pknA$::PknA	$mc^2\Delta pknA$ electroporated with pNit-PknA construct	This study
$mc^2\Delta pknA$::$PknA_{K42M}$	$mc^2\Delta pknA$ electroporated with pNit-$PknA_{K42M}$ construct	This study
$mc^2\Delta pknA$::$PknA_{KD}$	$mc^2\Delta pknA$ electroporated with pNit-$PknA_{KD}$ (aa 1–271) construct	This study
$mc^2\Delta pknA$::$PknA_{JM}$	$mc^2\Delta pknA$ electroporated with pNit-$PknA_{JM}$ (aa 1–341) construct	This study
$mc^2\Delta pknA$::$PknA_{TM}$	$mc^2\Delta pknA$ electroporated with pNit-$PknA_{TM}$ (aa 1–361) construct	This study
$mc^2\Delta pknA$::$PknA_{TATA}$	$mc^2\Delta pknA$ electroporated with pNit-$PknA_{TATA}$ (T172A,T174A) construct	This study
mc^2155::mCherry PknA	mc^2155 strain electroporated with pNit-mCherry PknA construct	This study
mc^2155::RFP-PknB	mc^2155 strain electroporated with pMV306-RFP-PknB construct; Hyg^r, Kan^r	Ref. 40
mc^2155::mCherry-$PknA_{K42M}$	mc^2155 strain electroporated with pNit-mCherry-$PknA_{K42M}$ construct	This study
mc^2155::$GFP_m{}^{2+}PknB_{K40M}$	mc^2155 strain electroporated with pNit-$GFP_m{}^{2+}$-$PknB_{K40M}$ construct	This study
H37Rv	Wild type *M. uberculosis* strain	ATCC
Rv-pptr-B	H37Rv *pknB* conditional mutant. *pknB* gene expression is under the regulation of pristinamycin inducible pptr promoter; Hyg^r.	Refs. 23 and 24
Rv-pptr-AB	H37Rv *pknA-pknB* conditional mutant. *pknA-pknB* expression is under the regulation of pristinamycin inducible pptr promoter; Hyg^r.	This study
Rv-pptr-AB::PknB	Rv-pptr-AB electroporated with integrative proficient pCiT-PknB, containing ATc-inducible PknB at L_5 site; Hyg^r & Cam^r	This study
Rv-pptr-AB::PknA-B	Rv-pptr-AB electroporated with integrative construct pCiT-PknA-B, containing ATc-inducible PknA-PknB at L_5 site	This study
Rv-pptr-AB::$PknA_{K42M}$-B	Rv-pptr-AB electroporated with integrative construct pCiT-$PknA_{K42M}$-B, containing ATc inducible $PknA_{K42M}$-PknB at attB site	This study
Rv-pptr-AB::$PknA_{KD}$-B	Rv-pptr-AB electroporated with integrative construct pCiT-$PknA_{KD}$PknB, containing ATc-inducible $PknA_{KD}$-PknB at attB site	This study
Rv-pptr-AB::$PknA_{JM}$-B	Rv-pptr-AB electroporated with integrative construct pCiT-$PknA_{JM}$-PknB, containing ATc-inducible $PknA_{JM}$-PknB at attB site	This study
Rv-pptr-AB::$PknA_{TM}$-B	Rv-pptr-AB electroporated with integrative construct pCiT-$PknA_{TM}$-PknB, containing ATc-inducible $PknA_{TM}$-PknB at attB site	This study
Rv-pptr-AB::$PknA_{T172A}$-B	Rv-pptr-AB electroporated with integrative construct pCiT-$PknA_{T172A}$-PknB, containing ATc-inducible $PknA_{T172A}$-PknB at attB site	This study
Rv-pptr-AB::$PknA_{T174A}$-B	Rv-pptr-AB electroporated with integrative construct pCiT-$PknA_{T174A}$-PknB, containing ATc-inducible $PknA_{T174A}$-PknB at attB site	This study
Rv-pptr-AB::$PknA_{T180A}$-B	Rv-pptr-AB electroporated with integrative construct pCiT-$PknA_{T180A}$-PknB, containing ATc-inducible $PknA_{T180A}$-PknB at attB site	This study
Rv-pptr-AB::$PknA_{TATA}$-B	Rv-pptr-AB electroporated with integrative construct pCiT-$PknA_{TATA}$-PknB, containing ATc-inducible $PknA_{TATA}$-PknB at B site	This study
Rv-pptr-AB::$PknA_{T3A}$-B	Rv-pptr-AB electroporated with integrative construct pCiT-$PknA_{T3A}$-PknB, containing ATc-inducible $PknA_{T3A}$-PknB at attB site	This study
Rv-pptr-AB::$PknA_{T224A}$-B	Rv-pptr-AB electroporated with integrative construct pCiT-$PknA_{T224A}$-PknB, containing ATc-inducible $PknA_{T224A}$-PknB at attB site	This study
Rv-pptr-AB::$PknA_{M3}$-B	Rv-pptr-AB electroporated with integrative construct pCiT-$PknA_{M3}$-PknB, containing ATc-inducible $PknA_{M3}$-PknB at attB site	This study

(~70 aa), the extracytoplasmic domain of PknB contains iterative penicillin-binding protein and serine/threonine kinase-associated (PASTA) domains (15, 21). Based on transposon mutagenesis, both PknA and PknB have been thought to be essential (22). Although PknB has been demonstrated to be essential both for *in vitro* growth and *in vivo* survival (23, 24), to date, there are no reports addressing the question of whether PknA is essential for growth or survival.

PknA and -B phosphorylate a number of proteins required for mycolic acid synthesis, cell division, and peptidoglycan synthesis (25–28). Despite the fact that many of their substrates were initially identified as substrates for one kinase or the other, most are actually phosphorylated by multiple kinases (27, 29, 30). PknB and PknH have recently been proposed to be the master regulators that are capable of phosphorylating seven STPKs in their activation loops *in vitro*, thus controlling their activation status (31). Based on the results from *in vitro* kinase assays, PknB has been suggested to activate four kinases (including PknA), which in turn phosphorylate their target substrates (31). It is conceivable that PknB, which participates in similar functions as PknA may regulate activation and functioning of PknA *in vivo*, akin to the cross-talk seen in most eukaryotic signaling pathways (19, 31). The mode of PknA activation in mycobacteria and its dependence on PknB have not been examined thus far. The present study investigates the functional importance of PknA *in vivo*. Using *Mycobacterium tuberculosis* conditional mutants to infect the mouse host, we find that PknA is essential for the survival of the pathogen both *in vitro* and *in vivo*.

MATERIALS AND METHODS

Bacterial Strains, Reagents, and Radioisotopes—A complete list of the bacterial strains used in the study is given in Table 1. Cloning and expression vector pMAL-c2x (New England Biolabs); *Escherichia coli* and mycobacterial shuttle plasmids pST-Hi, pST-HiT, pST-HiA, and pST-CiT (laboratory-generated vectors (32)); pNit-1 vector (33); pJAM2 (34); pVR1 shuttle plasmid (35); and p2Nil and pGOAL17 (36) vectors were procured from their respective sources. For fluorescence imaging, mCherry and $GFP_m{}^{2+}$ tags were amplified from pCherry3 (37) (Addgene-24659) and pMN437 (38) (Addgene-32363), respectively. Restriction endonucleases and DNA-modifying enzymes

were procured from New England Biolabs and MBI Fermentas. [γ-^{32}P]ATP (6000 Ci/mmol) was purchased from PerkinElmer Life Sciences. Pristinamycin 1A was purchased from Molcan Corp. (Richmond Hill, Canada), and the pENTR/D-TOPO kit was purchased from Life Technologies, Inc. Medium components were purchased from BD Biosciences. DNA oligonucleotides and analytical grade chemicals and reagents were purchased from Sigma-Aldrich or GE Healthcare, and Thr(P) antibodies were procured from Cell Signaling Technology.

Generation of Plasmid Constructs—Full-length *pknA* was amplified from BAC clone *Rv13* (a kind gift from Prof. Stewart Cole) using gene-specific primers and Phusion DNA polymerase (New England Biolabs). The gene was cloned into NdeI-HindIII sites in pNit vector, BamHI-XbaI sites in pJAM2 vector, and EcoRI-HindIII sites in pMAL-c2X vector to generate pNit-PknA, pJAM-PknA, and pMAL-PknA, respectively. pST-HiA-PknA construct was generated by subcloning *pknA* along with acetamide promoter from pJAM-PknA, using SspI-HindIII, into ScaI-HindIII sites of pST-Hi vector (32). In order to create PknA deletion mutants, amplicons generated using appropriate forward and reverse primers were cloned into NdeI-HindIII sites in pNit vector. PknA point mutations were generated by overlapping PCRs.

The integration-proficient shuttle vector pST-HiT with anhydrotetracycline (ATc)-inducible promoter was modified to create pST-CiT vector by replacing the hygromycin resistance gene (*hyg*^{r}) with the chloramphenicol resistance gene (*cam*^{r}) from pVR1 shuttle plasmid. *pknB* by itself or *pknA-pknB* together were amplified using specific primers and cloned into pST-CiT vector to generate pCiT-PknB and pCiT-PknA-B. In the presence of ATc, the rescue construct pCiT-PknA-B would express a bicistronic mRNA transcript. To create pCiT-PknA$_{mutant}$-B constructs, *pknA*$_{mutant}$ (such as PknA$_{K42M}$) and the functional *pknB* gene were cloned into pST-CiT vector. To create *pknA* deletion mutants (such as PknA$_{KD}$), a stop codon was introduced to terminate the translation at the designated codon. The veracity of the clones was confirmed through DNA sequencing.

Generation of Conditional Depletion Strain in M. tuberculosis and Mycobacterium smegmatis—The 5′ region of *pknA* (bp −20 to 750) was amplified from H37Rv genomic DNA, and the amplicon was cloned into the NcoI site in pAZI9479 (23), which does not contain mycobacterial origin of replication, to create the suicide delivery construct pAZ-PknA. The pAZ-PknA plasmid was electroporated into H37Rv, and the colonies were selected on 7H10 agar plates containing hygromycin (100 μg/ml) and pristinamycin (1.5 μg/ml). Genomic DNA was isolated from potential mutants and screened using specific primers (Fig. 1*A*) to confirm genuine recombination at the genomic locus.

M. smegmatis mc^{2}155 was electroporated with pHiA-PknA construct to create a merodiploid strain mc^{2}155-HiA-PknA. Approximately 1 kb upstream and downstream, flanking sequences of *pknA* were amplified using appropriate primers and cloned into pENTR-D-TOPO vector. pENTR-PknA-U (upstream flank) and pENTR-PknA-D (downstream flank) constructs were digested with HpaI-EcoRI and EcoRI-HindIII, respectively, and the flanks were cloned between the HpaI and HindIII sites in p2Nil vector. This was followed by cloning the 6-kb *hyg/sacB* cassette amplified from pGOAL17 at the PacI site, generating plasmid p2Nil-Δ*pknA*. The two-step homologous recombination technique (36) was employed to delete the genomic copy of *pknA*$_{smeg}$. Genomic DNA was isolated from potential mutants and screened for deletion at the genomic locus by PCR amplification across the deletion junctions.

Analysis of Growth Patterns—The Rv-pptr-AB mutant was transformed with pCiT-PknB or pCiT-PknA-B plasmids by electroporation to create Rv-pptr-AB::PknB or Rv-pptr-AB::PknA-B strains, where expression of *pknB* or *pknA-pknB* is under the regulation of an ATc-inducible promoter. To analyze the growth patterns of mutant cell types, liquid cultures of Rv-pptr-AB and the transformants were grown in 7H9 broth (containing ADC, 0.1% Tween 80, 0.2% glycerol, 1.5 μg/ml pristinamycin, and appropriate antibiotics) to A_{600} of 0.8. The cells were washed twice with phosphate-buffered saline, pH 7.4 (PBS) containing 0.05% Tween 80 (PBST) to remove traces of pristinamycin and diluted to A_{600} of 0.1; the cultures were grown either in the absence or presence of pristinamycin for 6 days; and the absorbance was measured every 24 h. For replica plating experiments, cultures washed with PBS were diluted to A_{600} of 0.2 in fresh 7H9 broth. 5 μl of each cell suspension was streaked onto 7H10 agar plates containing either 1.5 μg/ml pristinamycin or 1.5 μg/ml ATc. These plates were incubated at 37 °C for 20–24 days. For complementation experiments, Rv-pptr-AB was transformed with pCiT-PknB, pCiT-PknA-B, or various pCiT-PknA$_{mutant}$-B constructs. The growth patterns of transformants were analyzed as described above. To determine whether the absence of PknA has bactericidal or bacteriostatic effects, cultures were withdrawn on days 0, 2, 4, and 6, serially diluted, and spotted on plates containing pristinamycin 1A. Inducers pristinamycin and ATc were used at concentrations of 1.5 μg/ml under growth and starvation conditions. To determine the viability of the strains in the presence of PknA$_{mutants}$ (such as PknA$_{TM}$ or PknA$_{TATA}$), cultures were grown in presence of ATc for 4 days, serially diluted in fresh 7H9, and plated on pristinamycin-containing plates. cfu were determined after incubation.

The mc^{2}Δ*pknA* mutant was electroporated with pNit vector or pNit-PknA or pNit-PknA$_{mutant}$ construct to generate mc^{2}Δ*pknA*::pNit, mc^{2}Δ*pknA*::pNit-PknA, or mc^{2}Δ*pknA*::pNit-PknA$_{mutant}$ strains, respectively. These strains were grown in Luria-Bertani (LB) broth containing 0.2% glycerol, 0.05% Tween 80, and 0.5% acetamide in the presence of the antibiotics hygromycin (100 μg/ml) and kanamycin (25 μg/ml) to A_{600} of 0.8–1.0. The cells were harvested and washed thoroughly in PBST buffer twice to remove traces of acetamide. The cultures were initiated at A_{600} 0.05 in fresh LB broth (containing Tween 80 with 0.2% glycerol), 0.2 μM isovaleronitrile (IVN), and appropriate antibiotics. The growth pattern was analyzed in triplicates by monitoring changes in cell density spectrophotometrically at A_{600} every 3 h.

Western Blot Analysis—Cultures of *M. smegmatis* strains were initiated at A_{600} of 0.3 and were grown in the absence or presence of acetamide or IVN for 3 h. Cultures of *M. tuberculosis* strains were initiated at A_{600} of 0.2 and grown in the absence or presence of pristinamycin or ATc for 4 days. Cell-

free extracts were prepared using a bead beater to lyse cells, followed by high speed centrifugation to clarify the extracts. The protein concentrations of lysates were estimated using the Bradford method. Lysates were probed with antibodies against PknA, PknB, PstP, and GroEL1 in standard Western blotting experiments. The PstP antibodies were a kind gift from Dr. Yogendra Singh (CSIR-Institute of Genomics and Integrative Biology), and the PknA, PknB, and GroEL1 antibodies were raised in our laboratory.

Scanning Electron Microscopy—Cultures of H37Rv, Rv-pptr-AB, and Rv-pptr-AB::PknB grown in the presence of either pristinamycin or ATc were fixed in fixative solution (4% paraformaldehyde and 2.5% glutaraldehyde in 0.1 M sodium cacodylate buffer, pH 7.3) by mixing culture and fixative in a 1:1 ratio for 10 min. Cells were pelleted down, resuspended in 5 ml of fixative, and kept at 4 °C for 1 h, followed by overnight incubation at room temperature. Fixed cells were processed, and scanning electron microscopy images were obtained at 20,000 × using a Carl Zeiss Evo LS scanning electron microscope, as described earlier (24).

Expression and Purification of Proteins and in Vitro Kinase Assay—pMAL-c2X constructs expressing PknA and its mutants were transformed into *E. coli* BL21 (DE3) Codon Plus cells (Stratagene), and the MBP-tagged proteins were purified as described (27). An *in vitro* kinase assay was performed as described previously (39) using PknA kinase or its mutants (2.5 pmol) and myelin basic protein (100 pmol) as the substrate.

Characterization of Phospho-specific Antibodies—The phospho-specific antibodies used in this study were custom made by PhosphoSolutions, Inc. (Aurora, CO) against the dually phosphorylated peptide ^{168}[C]AAPVpTQpTGMV^{177} (where pT represents phosphothreonine). To characterize and validate the specificity of phospho-specific PknA antibodies, *E. coli* BL21 strain was transformed with pMAL-PknA or pMAL-$PknA_{mutant}$ constructs. Expression of PknA or $PknA_{mutant}$ proteins was induced with 1 mM isopropyl 1-thio-β-D-galactopyranoside at 18 °C for 12 h. Cells were lysed in 2× SDS-sample buffer, and equivalent lysates were resolved and probed with probed with anti-PknA, anti-Thr(P), and anti-p-PknA antibodies. To determine the ability of the anti-p-PknA antibodies to specifically detect PknA expressed in mycobacteria, WCLs from mc^{2}Δ*pknA*::pNit, mc^{2}Δ*pknA*::pNit-PknA, mc^{2}Δ*pknA*::pNit-$PknA_{K42M}$, and mc^{2}Δ*pknA*::pNit-$PknA_{TATA}$ were probed with anti-PknA, anti-GroEL1, anti-PknB, and anti-p-PknA antibodies. To determine the influence of PknB on loop phosphorylation of PknA, WCLs prepared from H37Rv or Rv-pptr-B (23, 24) in the presence or absence of inducer pristinamycin were probed with anti-PknA, anti-GroEL1, anti-PknB, and anti-p-PknA antibodies.

Fluorescence Microscopy—The genes encoding GFP_m^{2+} and mCherry fluorophores were amplified from plasmids pMN437 and pCherry3, respectively. The *mCherry* amplicon was digested with NdeI and SapI, and the amplicons of *pknA* or $pknA_{K42M}$ were digested with SapI and HindIII. Fusion genes were created in a three-piece ligation involving the two amplicons and plasmid pNit digested with NdeI-HindIII, to generate plasmid pNit-mCh-PknA or pNit-mCh-$PknA_{K42M}$. A similar strategy was employed for generating pNit-GFP_m^{2+}-$PknB_{K40M}$. The pMV306-RFP-PknB construct was a kind gift from Dr. Robert Husson (40). Overnight cultures of *M. smegmatis* mc^{2}155 strains transformed with one or the other of the above plasmids were used to initiate fresh cultures at an A_{600} of 0.1 and grown in the presence of 1.0 μM IVN or 0.2% acetamide at 30 °C to A_{600} of 0.8–1.0 in order to express fluorophore-tagged PknA or PknB, respectively. Cells were harvested, washed twice with PBS, and fixed with 4% paraformaldehyde (v/v) for 30 min at room temperature. The cells were then washed with PBS again, and the harvested cells were stored in the dark at 4 °C. Vancomycin FL labeling was performed as described previously (41). Cells were visualized using a Nikon microscope with a ×100 differential interference contrast oil immersion objective with green and red fluorescence filters. Monochrome images were acquired using DS-Qi2 and NIS-Elements and processed using Adobe Photoshop.

Infection of Mice—*M. tuberculosis* H37Rv, Rv-pptr-AB::PknB, or Rv-pptr-AB::PknA-B was grown in the presence of pristinamycin until A_{600} of 0.6. The bacilli were prepared as described previously (24). C57BL/6 mice of either sex (6–8 weeks old) obtained from the breeding facility at the National Institute of Immunology were housed in individually ventilated cages at the Tuberculosis Aerosol Challenge Facility (TACF), International Center for Genetic Engineering and Biotechnology (ICGEB) (New Delhi, India) and cared for as per the established animal ethics and guidelines. Mice ($n = 6$) were infected with 2×10^8 colony forming units of either H37Rv, Rv-pptr-AB::PknB, or Rv-pptr-AB::PknA-B by the aerosol route as described previously (24).

Bacillary load in the lungs was determined 24 h postinfection to confirm the implantation of the dosage administered. Bacterial loads were determined both from the lung and spleen 4 and 8 weeks postinfection as described earlier (24) to determine the extent of infection and pathogen survival. For histopathological evaluation, harvested organs were fixed in 10% neutral buffered formalin and processed as described previously (24). Each granuloma was graded using the following criteria: (*a*) granulomas with necrosis were given a score of 5; (*b*) granulomas without necrosis were given a score of 2.5; and (*c*) granulomas with fibrous connective tissue were given a score of 1. The total granuloma score was calculated by multiplying the number of granulomas of each type by the score and then summing them up to obtain a total granuloma score for each sample.

RESULTS

Creation of M. tuberculosis pknA-pknB Conditional Mutant—We have earlier demonstrated (24) that PknB is essential for growth and survival of the pathogen both *in vitro* and *in vivo*. To determine the role of PknA in growth and survival of the pathogen and the role of PknB in modulating PknA-mediated signaling, we adopted the route of creating conditional mutants and analyzing their phenotypes. We first generated an *M. tuberculosis* H37Rv conditional mutant wherein the transcription of both *pknA* and *pknB* genes was placed under the control of a pristinamycin-inducible promoter (pptr). Toward this, we used the suicide delivery plasmid pAZ-PknA to modify *pknA* at its genomic locus by introducing an inducible *pptr* promoter upstream (Fig. 1*A*). *M. tuberculosis* H37Rv was transformed

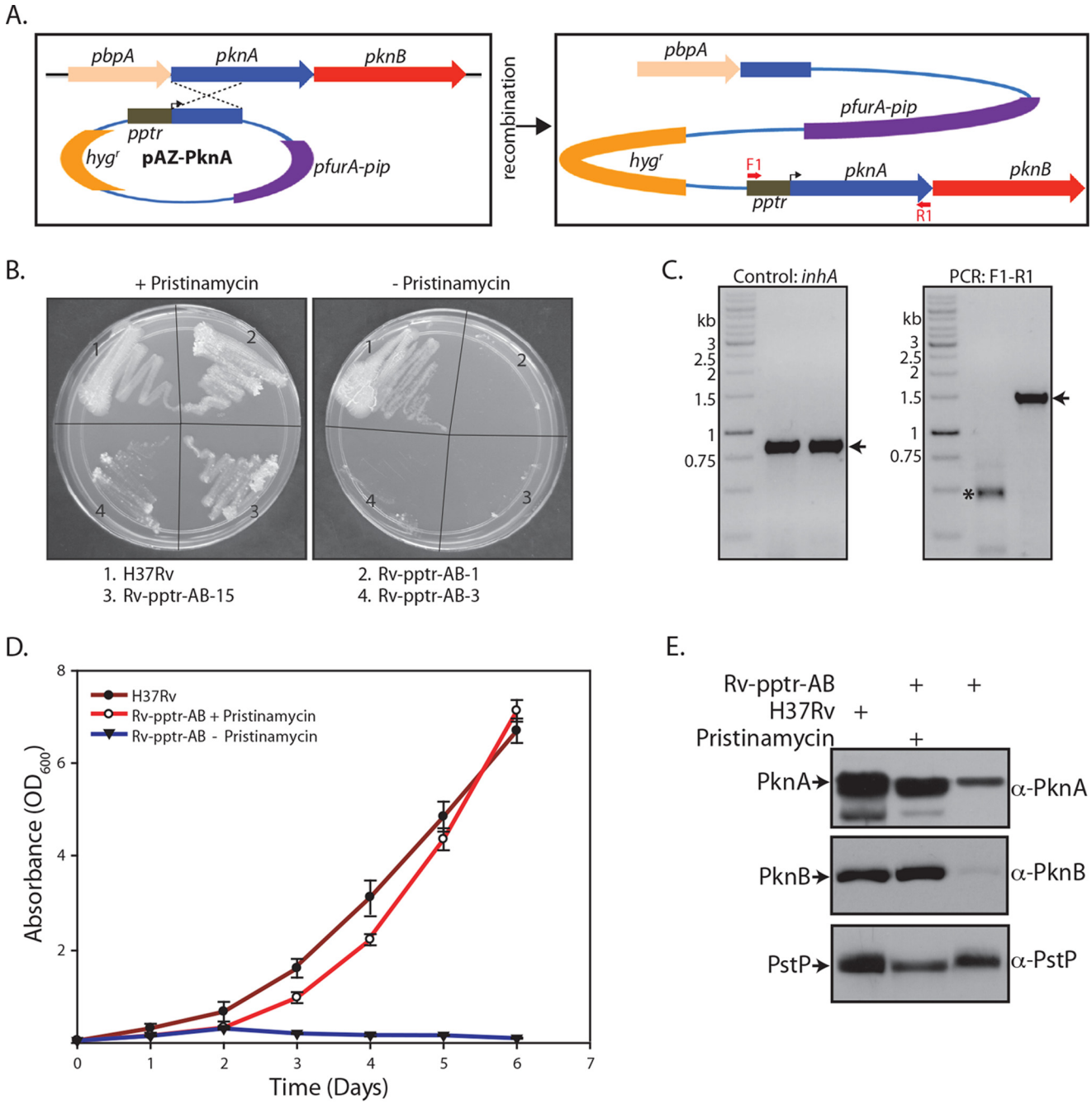

FIGURE 1. **Creation of *M. tuberculosis* pknA-pknB conditional mutant.** *A*, schematic representation of the strategy for generation of Rv-pptr-AB mutant. *M. tuberculosis* H37Rv (*H37Rv*) was electroporated with 5 μg of pAZ-PknA construct, and after recovery, the cells were plated on plates containing hygromycin and pristinamycin. Primers used for PCR confirmation are depicted by *red arrows* (*F1* and *R1*). *B*, cultures of H37Rv and Rv-pptr-AB clones 1, 15, and 3, were streaked on 7H10 agar plates in the presence or absence of 1.5 μg/ml pristinamycin. *C*, agarose gels showing PCR products following PCR amplification using genomic DNA of *M. tuberculosis* H37Rv and Rv-pptr-AB conditional mutant. *Left*, PCR amplification of positive control, 0.85-kb *inhA* gene, using a gene-specific primer set. *Right*, PCR amplification of altered locus using pptr promoter primer, F1, and *pknA* reverse primer, R1. The appearance of a 1.5-kb PCR amplicon (indicated by an *arrow*) in *lane 2* confirms the recombination. *Asterisk*, nonspecific band in *lane 1*. *D*, *in vitro* growth analysis of wild type H37Rv and Rv-pptr-AB in the presence or absence of pristinamycin. All the cultures were seeded at an initial A_{600} of 0.1. The experiment was performed in triplicates, and the mean is presented with *error bars*. *Error bars*, S.E. *E*, H37Rv and Rv-pptr-AB cultures were seeded at an initial A_{600} of 0.2. WCLs prepared from cultures grown in the presence or absence of pristinamycin, as indicated, for 4 days were resolved and probed with rabbit polyclonal α-PknA, α-PknB, and α-PstP antibodies.

with pAZ-PknA, and the transformants were selected for, in the presence of inducer pristinamycin. Growth patterns were analyzed by streaking wild type (H37Rv) and three potential mutants on 7H10 agar plates in the presence or absence of pristinamycin. Although H37Rv grew both in the presence and absence of inducer, all three potential mutants grew only in the presence of pristinamycin, suggesting that they are likely to be genuine mutants (Fig. 1*B*). Analysis of amplicons obtained by PCR across the replacement junctions confirmed that site-specific recombination had occurred at the native locus of *pknA* (Fig. 1*C*). Examination of the growth kinetics of the mutants in liquid culture revealed marginal differences between H37Rv and Rv-pptr-AB in the presence of pristinamycin. However, in the absence of inducer, the growth of Rv-pptr-AB strain was

dramatically compromised (Fig. 1*D*). *pknA* and *pknB* genes are the terminal genes of an operon that carries three other genes, including the sole serine/threonine phosphatase *pstP*. We compared the expression of *pknA* and *pknB* in the presence and absence of inducer with expression of *pstP*, the first gene of the operon. Whereas the expression of both PknA and PknB was drastically compromised in the absence of inducer, expression of PstP was unaltered (Fig. 1*E*). These results authenticate the creation of a conditional gene replacement mutant of *pknA-pknB* in *M. tuberculosis* H37Rv.

pknA Depletion in M. smegmatis and M. tuberculosis Results in Cell Death—To delineate the role of PknA in mycobacteria, we developed a conditional depletion strain of *pknA* in *M. smegmatis* and *M. tuberculosis*. Toward generating an *M. smegmatis* conditional mutant, we integrated an inducible copy of $pknA_{tb}$ in the genome prior to deleting the gene at its native locus (Fig. 2*A*). Analysis of differential sized amplicons obtained by PCR with different primer combinations (indicated in Fig. 2*A*) confirmed deletion of $pknA_{smeg}$ at its genomic locus. We found that the growth of $mc^2\Delta pknA$ did not significantly diverge from the corresponding wild type strain in the presence of acetamide. However, depletion of PknA in the $mc^2\Delta pknA$ strain resulted in severely compromised growth (Fig. 2*B*). Western blot analysis in the presence or absence of inducer showed effective depletion of PknA, whereas the levels of PknB, PstP, and GroEL1 remained unaltered (Fig. 2*C*). In order to create a conditional mutant of *pknA* in *M. tuberculosis*, we transformed the Rv-pptr-AB strain with the integration-proficient pCiT-PknB or pCiT-PknA-B constructs, in which *pknB* or *pknA-pknB* together were cloned under an ATc-inducible promoter, to generate Rv-pptr-AB::PknB and Rv-pptr-AB::PknA-B strains (Fig. 2*D*). In the absence of pristinamycin and upon the addition of ATc, Rv-pptr-AB::PknB would be equivalent to a *pknA* mutant strain, and Rv-pptr-AB::PknA-B, would be comparable with a complemented strain. Growth was analyzed by replica streaking the H37Rv, Rv-pptr-AB::PknB, and Rv-pptr-AB::PknA-B strains on plates containing either pristinamycin or ATc. Whereas H37Rv and Rv-pptr-AB::PknA-B grew normally on both pristinamycin and ATc plates, Rv-pptr-AB::PknB failed to survive on ATc plates. Western blot analysis of Rv-pptr-AB::PknB grown in the presence of ATc showed effective depletion of PknA, whereas expression of PknB and GroEL1 remained unaltered (Fig. 2*E*, compare *lanes 4* and *5*). Although the protein levels of both PknA and PknB detected in Rv-pptr-AB::PknA-B strain were lower compared with Rv-pptr-AB strain, no change in the levels of either PknA or PknB was observed in the absence or presence of inducer (Fig. 2*E*, compare *lanes 6* and *7*). These results clearly demonstrate PknA to be independently essential for *M. tuberculosis* growth and survival *in vitro* (Fig. 2, *D* and *E*).

PknA Depletion in M. tuberculosis Results in Aberrant Cell Morphology—Although growth in the absence of PknA was evidently compromised, we could not determine whether the depletion of PknA was leading to a bacteriostatic or bactericidal phenotype. To address this question, H37Rv, Rv-pptr-AB, and Rv-pptr-AB::PknB cultures grown in the presence or absence of either pristinamycin or ATc (as indicated in Fig. 3*A*) for 0, 2, 4, or 6 days were serially diluted and spotted on plates containing pristinamycin. Depletion of PknA or both PknA and PknB for 2 days had no apparent effect on cell growth, indicating that the cells could recover after 2 days of depletion. Interestingly, upon 4 days of depletion, we observed a growth difference of ~3–4 orders of magnitude in the case of depletion of both PknA and PknB and a growth difference of ~2 orders of magnitude in the case of PknA depletion alone. This trend continued, with PknA and PknB depletion leading to almost complete clearance (growth difference of ~5 orders of magnitude) and PknA depletion leading to growth lowered by ~4 orders of magnitude after 6 days of depletion (Fig. 3*A*). These results strongly suggest that depletion of PknA alone eventually leads to cell death. Importantly, depletion of both PknA and PknB seems to have a cumulative impact on the cell survival.

We investigated the morphological changes associated with depletion of either PknA or both PknA and PknB using scanning electron microscopy. Compared with H37Rv, Rv-pptr-AB cells showed slightly elongated morphology in the presence of pristinamycin (Fig. 3*B*, *left panels*). Conditional depletion of PknA for 2 days resulted in elongated cells with marginally shriveled cell morphology (indicated). After 4 days of growth in the absence of PknA (Rv-pptr-AB::PknB), cells were severely affected, with most of the cells fused to each other and almost at the brink of lysis. In the absence of both PknA and PknB, a more radical phenotype was observed; although the cells were similar in length to that of H37Rv, within 2 days of depletion, cells appeared shriveled and sickly, and some of the cells were fused to each other. After 4 days of depletion, almost all of the cells were fused to each other, and we observed substantial cell lysis (Fig. 3*B*). We have previously shown that similar morphological patterns were observed upon PknB depletion in *M. smegmatis* (24). Taken together, the loss of PknA or PknB either independently or together alters the cell morphology, eventually leading to cell death.

PknA Is Indispensable for Survival of the Pathogen in the Host—We evaluated the importance of PknA for survival of *M. tuberculosis* in the host using the murine infection model. Toward this, C57BL/6 mice were infected with H37Rv, Rv-pptr-AB::PknB or Rv-pptr-AB::PknA-B strains grown in the presence of pristinamycin, through the aerosol route. After the infection, all of the mice were provided with doxycycline-containing water to induce the expression of PknB or PknA-B from the tetracycline-inducible promoter. Thus, mice infected with Rv-pptr-AB::PknB would behave akin to a PknA mutant, and mice infected with Rv-pptr-AB::PknA-B would be equivalent to a complemented strain. The cfu counts obtained in the lungs of infected mice after 24 h revealed that the number of implanted bacilli were similar for all three strains (Fig. 4*B*). Whereas the lungs of mice infected with H37Rv and Rv-pptr-AB::PknA-B showed discrete bacilli spread throughout the lung and spleen at both 4 and 8 weeks postinfection, the spleen of mice infected with Rv-pptr-AB::PknB manifested significantly reduced inflammation (Fig. 4*A*). Furthermore, the enlargement of spleen (splenomegaly) observed at both 4 and 8 weeks postinfection followed the same trend (Fig. 4*C*). The bacillary load in the lung of mice infected with wild type (H37Rv) and Rv-pptr-AB::PknA-B (PknA-B-complemented) strains were similar at both 4 and 8 weeks postinfection (Fig. 4*B*). Despite

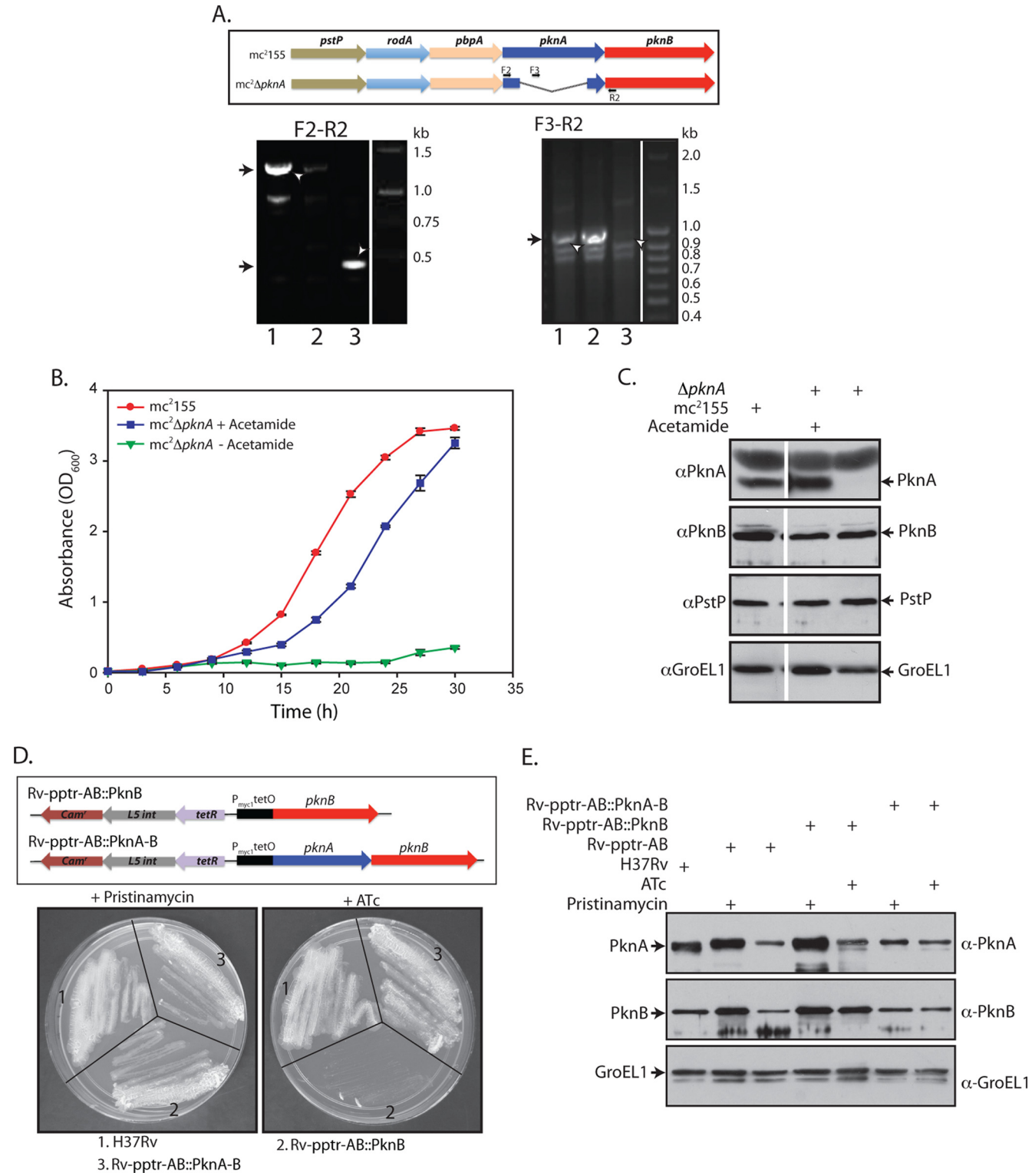

FIGURE 2. **PknA depletion in *M. smegmatis* and *M. tuberculosis* results in cell death.** *A*, *top*, pictorial representation of the genomic region in *M. smegmatis* mc²155 and mc²Δ*pknA* conditional gene replacement strain, showing the internal deletion in native *pknA*. Primers used for PCR amplification are depicted. *Bottom*, agarose gels showing the PCR amplification using genomic DNA of *M. smegmatis* mc²155, mc²155-HiA-PknA, and mc²Δ*pknA* in *lanes 1–3*, respectively. *Left*, differential PCR amplicons obtained in mc²155 and mc²155-HiA-PknA *versus* mc²Δ*pknA* (*white arrowheads*) using F2-R2 primers. *Right*, absence of ~1.0-kb PCR amplicon in mc²Δ*pknA* using F3-R2 primers (*white arrowheads*; compare *lane 3* with *lanes 1* and *2*). *B*, *in vitro* growth pattern analysis of *M. smegmatis* mc²155 and mc²Δ*pknA* mutant in the presence or absence of acetamide. All of the cultures were seeded at an initial A_{600} of 0.02. *Error bars*, S.E. *C*, mc²155 and mc²Δ*pknA* grown in the presence of acetamide were seeded at A_{600} of 0.3 and grown for 3 h in the presence or absence of acetamide. WCLs were resolved and probed with α-PknA, α-PknB, α-PstP, and α-GroEL1 antibodies. *D*, *top*, schematic representation of Rv-pptr-AB strain complemented with integration proficient plasmid pCiT-PknB or pCiT-PknA-B to generate Rv-pptr-AB::PknB and Rv-pptr-AB::PknA-B, respectively. *Bottom*, log phase cultures of H37Rv, Rv-pptr-AB::PknB, and Rv-pptr-AB::PknA-B were replica-streaked on 7H10 agar plates containing 1.5 μg/ml of either pristinamycin or ATc. *E*, H37Rv, Rv-pptr-AB, Rv-pptr-AB::PknB, or Rv-pptr-AB::PknA-B was grown to an A_{600} of 0.8 in the presence of pristinamycin were used to seed fresh cultures at an initial A_{600} of 0.2. H37Rv, Rv-pptr-AB, Rv-pptr-AB::PknB, and Rv-pptr-AB::PknA-B cultures were grown in the presence or absence of pristinamycin or ATc as indicated for 4 days. WCLs were resolved and probed with α-PknA, α-PknB, and α-GroEL1 antibodies.

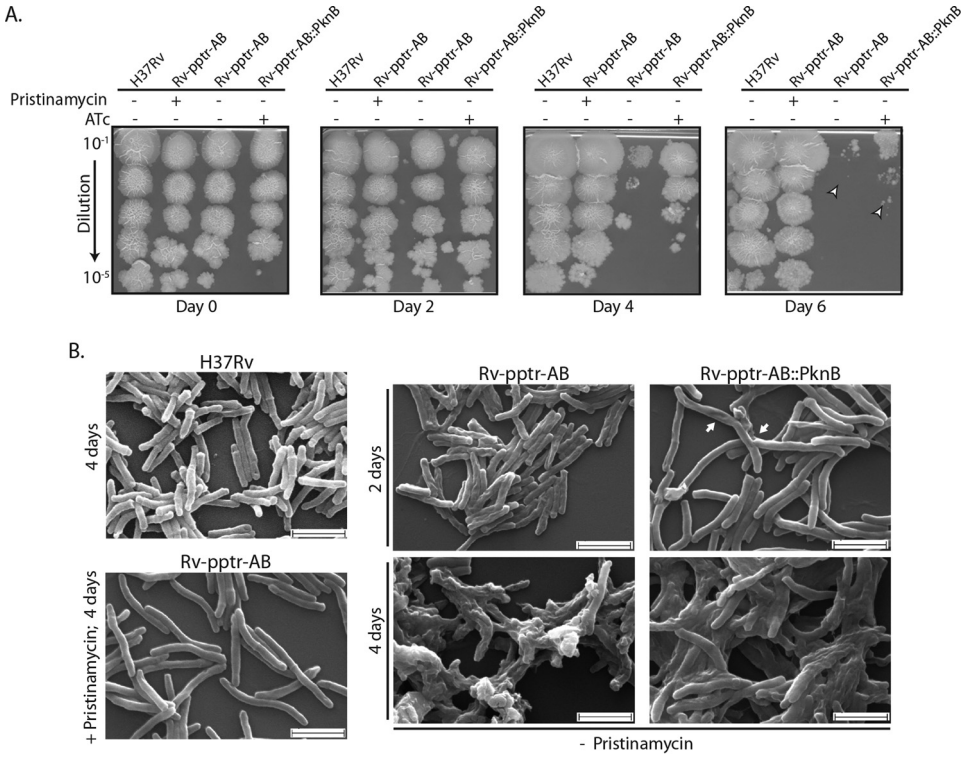

FIGURE 3. **PknA depletion in *M. tuberculosis* results in aberrant cell morphology.** *A*, H37Rv, Rv-pptr-ABm, and Rv-pptr-AB::PknB grown to an A_{600} of 0.8 in the presence of pristinamcyin were used to seed fresh cultures at an initial A_{600} of 0.1. H37Rv, Rv-pptr-AB, and Rv-pptr-AB::PknB cultures were grown either in the presence or absence of pristinamycin or ATc, as indicated, for 0, 2, 4, or 6 days. Cultures at each time point were serially diluted and spotted on 7H10 agar plates containing pristinamycin. *B*, morphology of H37Rv, Rv-pptr-AB, and Rv-pptr-AB::PknB observed through scanning electron microscopy. H37Rv, Rv-pptr-AB, and Rv-pptr-AB::PknB cultures were seeded at A_{600} of 0.1, and H37Rv was grown for 4 days in the absence of any inducer. Rv-pptr-AB cultures were grown either in the presence or absence of pristinamycin for 2 and 4 days, as indicated. Cultures of Rv-pptr-AB::PknB were grown in the presence of ATc (in the absence of pristinamycin) for 2 and 4 days. *Scale bar*, 2 μm.

incubating the plates for prolonged periods, however, we did not detect any colonies from the lungs of mice infected with Rv-pptr-AB::PknB strain at both time points (Fig. 4*B*). The cfu data obtained for the spleen of the infected mice were in accordance with the lung data (Fig. 4*D*).

We then assessed the gross pathological changes in the tissues obtained from the lungs of the mice at 8 weeks postinfection. The gross observations were in accordance with the observed pulmonary and splenic bacillary loads (Figs. 4 (*B* and *D*) and 5*A*). Whereas the lungs of animals infected with wild type H37Rv or complemented strain (Rv-pptr-AB::PknA-B) displayed substantial infection with numerous large granulomatous architecture, in the lungs of animals infected with PknA mutant (Rv-pptr-AB::PknB), normal lung parenchyma was observed (Fig. 5*A*). The gross pathological score obtained based on lesions in lung tissue showed that wild type H37Rv infection caused more severe damage compared with the complemented strain (Fig. 5*B*). Histopathological analysis showed extensive damage in the wild type H37Rv-infected mice lung samples, and relatively less severe damage in the lungs of mice infected with the complemented strain Rv-pptr-AB::PknA-B (Fig. 5*C*). In contrast, the lungs of mice infected with PknA mutant strain showed normal microarchitecture, with infiltration of fewer leukocytes (Fig. 5*C*). Thus, our data suggest that PknA plays an indispensable role in bacterial pathogenesis, and its depletion leads to complete clearance of the pathogen from the host tissues.

The Extracellular Domain of PknA Is Dispensable for Cell Survival—The invariant lysine at position 42 (Lys^{42}) of PknA is required for interaction with ATP and has been shown to be critical for its *in vitro* activity (20). To investigate the importance of PknA activity for the growth of *M. smegmatis*, $mc^2\Delta pknA$ strain was transformed with pNit vector, pNit-PknA, or pNit-$PknA_{K42M}$. Although expression of PknA in $mc^2\Delta pknA$::pNit vector was found to be diminished in the absence of acetamide inducer (Fig. 6*B*, compare *lanes 2* and *3*), robust expression of wild type PknA and $PknA_{K42M}$ was observed in the presence of IVN (Fig. 6*B*). In the absence of inducer, $mc^2\Delta pknA$ transformed with pNit-PknA grew robustly, indicating that wild type PknA was capable of functional complementation (Fig. 6*C*). However, $mc^2\Delta pknA$ transformed with either the pNit vector or kinase inactive $PknA_{K42M}$ did not show growth recovery, therefore demonstrating the significance of PknA kinase activity for cell growth and survival (Fig. 6*C*). To investigate whether the same effects were detected in *M. tuberculosis*, Rv-pptr-AB was transformed with the pCiT-$PknA_{K42M}$-PknB construct to generate Rv-pptr-AB::$PknA_{K42M}$-B. Growth patterns of Rv-pptr-AB::PknB, Rv-pptr-AB::PknA-B, and Rv-pptr-AB::$PknA_{K42M}$-B were analyzed, and it was found that whereas Rv-pptr-AB::PknA-B grew on both pristinamycin or ATc plates, both Rv-pptr-AB::PknB and Rv-pptr-AB::$PknA_{K42M}$-B did not grow on ATc plates, confirming the essentiality of PknA kinase activity in PknA function and cell survival (Fig. 6*D*).

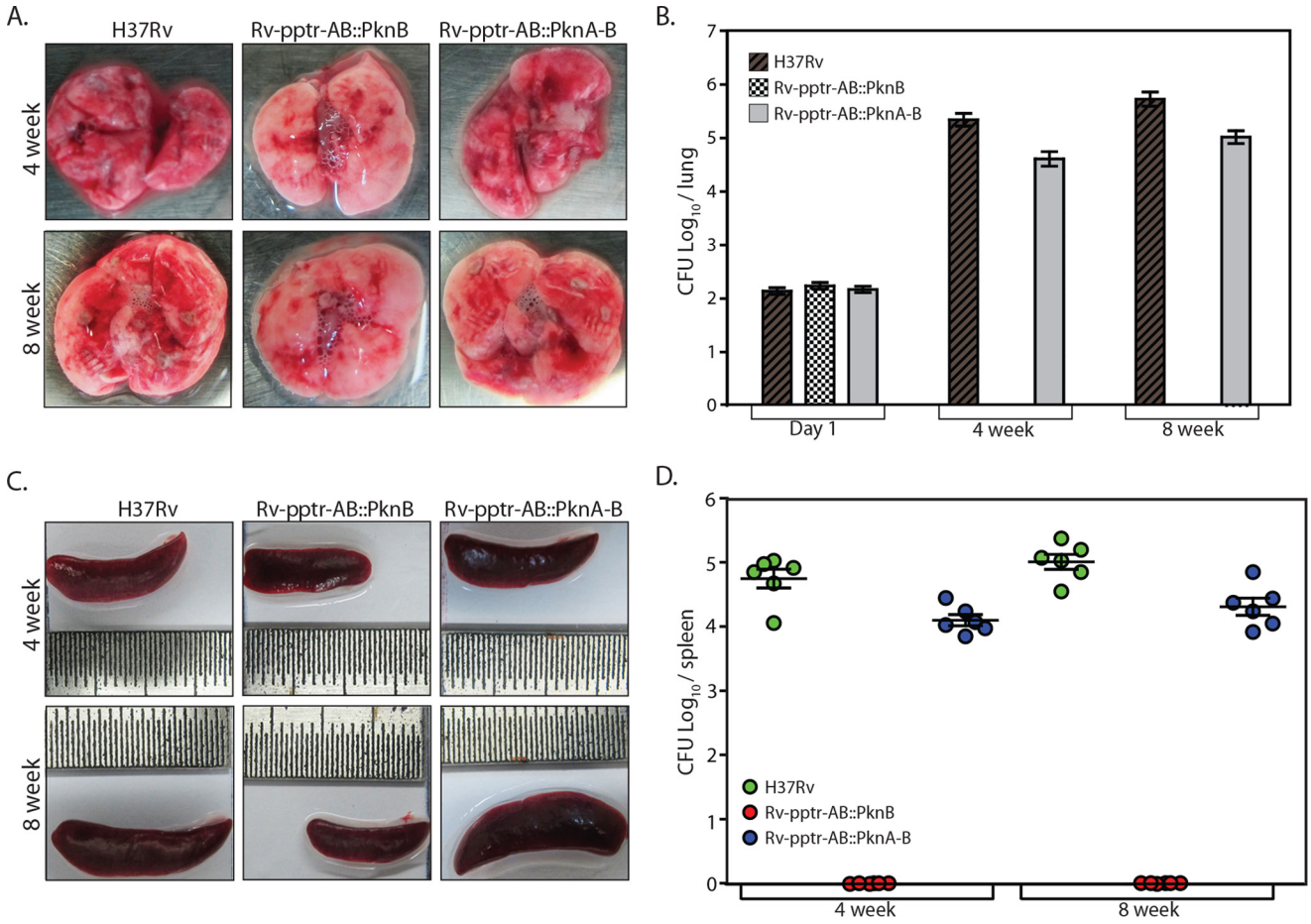

FIGURE 4. **PknA is indispensable for survival of the pathogen in the host.** *A* and *C*, representative images of lung and spleen from mice infected with 150–200 bacilli cfu of H37Rv or Rv-pptr-AB::PknB or Rv-pptr-AB::PknA-B after 4 and 8 weeks of infection. *B*, mice ($n = 2$) were sacrificed on day 1, and dilutions of lung homogenates were plated to determine the deposition of infected bacilli in the lung. 4 and 8 weeks postinfection, different dilutions of lung homogenates from the mice ($n = 6$) infected with different strains were plated to determine the bacterial load. At 4 weeks postinfection, the cfu for H37Rv-, Rv-pptr-AB::PknB-, and Rv-pptr-AB::PknA-B-infected mice were 5.34 $\log_{10}$, below the detection range, and 4.61 $\log_{10}$, respectively. The cfu for the mice infected with the above strains at the 8-week time point were 5.73 $\log_{10}$, below the detection range, and 5.01 $\log_{10}$. Results were plotted with cfu $\log_{10}$/lung on the *y* axis and time points on the *x* axis. *D*, splenic bacillary load for mice infected with H37Rv, Rv-pptr-AB::PknB, and Rv-pptr-AB::PknA-B at 4 and 8 weeks postinfection was 4.75 $\log_{10}$, below the detection range, and 4.10 $\log_{10}$ (4 weeks) and 5.03 $\log_{10}$, below the detection range, and 4.24 $\log_{10}$ (8 weeks), respectively. Results were plotted with cfu $\log_{10}$/spleen on the *y* axis and time points on the *x* axis. *Error bars*, S.E.

PknA protein has a length of 431 amino acids with a 271-aa N-terminal kinase domain (KD), a 68-aa juxtamembrane domain (JM), a 20-aa single helix transmembrane motif (TM), and a short 70-aa extracellular domain (Fig. 6*A*). *In vitro* kinase assays have shown that the intracellular region consisting of the kinase and juxtamembrane domains is catalytically active (42). To delineate the domains of PknA required for cell survival in mycobacteria, we generated deletion mutants $PknA_{KD}$ (aa 1–271), $PknA_{JM}$ (aa 1–341), and $PknA_{TM}$ (aa 1–361) in pNit and pCiT vectors (Fig. 6*A*). In *M. smegmatis* as well as *M. tuberculosis*, both $PknA_{KD}$ and $PknA_{JM}$ failed to complement cell growth upon depletion of PknA (Fig. 6, *F* and *G*). Interestingly, $PknA_{TM}$ (which lacks the extracytoplasmic domain) effectively complemented cell growth in the absence of full-length PknA, indicating that the extracytoplasmic domain is dispensable (Fig. 6, *F* and *G*). Because we could not detect the expression of the deletion mutants in the Rv-pptr-AB-complemented strains, we utilized the $mc^2\Delta pknA$ strain complemented with the pNit constructs expressing $PknA_{KD}$, $PknA_{JM}$, and $PknA_{TM}$ to detect the expression of the deletion mutants. Western blot analysis showed the expression of $PknA_{KD}$, $PknA_{JM}$, and $PknA_{TM}$, albeit at lower levels compared with the full-length PknA (Fig. 6*E*, *white arrowheads*). Next we analyzed the bacterial viability of Rv-pptr-AB::PknA-B and Rv-pptr-AB::$PknA_{TM}$-B grown in the presence of pristinamycin or ATc (Fig. 6*G*, *right*). Whereas the cfu obtained from Rv-pptr-AB::PknA-B grown in the presence of either pristinamycin or ATc were similar, cfu for Rv-pptr-AB::$PknA_{TM}$-B grown in the presence of ATc showed 2-fold reduced bacterial viability, probably due to lower expression levels of $PknA_{TM}$ mutant compared with PknA (Fig. 6*G*, *right*). Taken together, these results suggest that although PknA kinase activity is essential for cell survival, the extracellular domain is dispensable for PknA-mediated cell survival and growth.

Abrogation of Phosphorylation in the Activation Segment Affects Catalytic Activity of PknA—The activation of protein kinases is generally accomplished by the phosphorylation of one or more serine, threonine, or tyrosine residues in their activation loop, which lies between the conserved DFG and APE motifs (43) (Figs. 6*A* and 7*A*). Mutating either Thr^{172} or Thr^{174}

A.

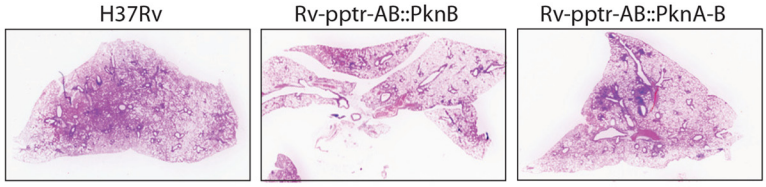

B.

Strain	No. of granulomas with necrosis Score: 5	No. of granulomas without necrosis Score: 2.5	No. of granulomas with fibrosis Score: 1	Total granuloma Score
H37Rv	0	7	0	17.5
Rv-pptr-AB::PknB	0	0	0	0
Rv-pptr-AB::PknA-B	0	3	0	7.5

C.

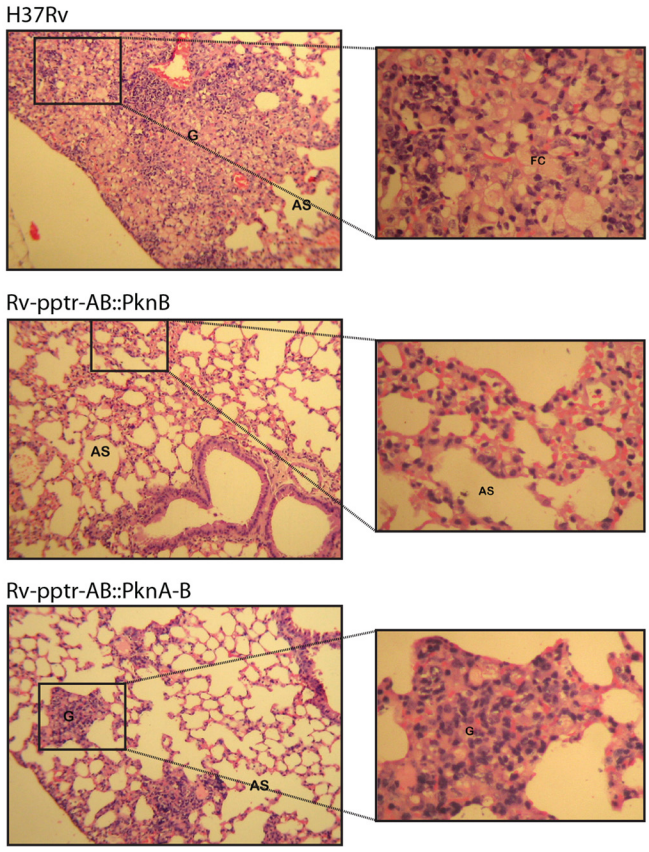

FIGURE 5. **Gross histopathological observations in the lungs of infected mice.** *A*, images shown are representative of typical lung sections obtained from mice infected with H37Rv, Rv-pptr-AB::PknB, and Rv-pptr-AB::PknA-B at 8 weeks postinfection. *B*, granuloma score calculated as described under "Materials and Methods" for H&E-stained lung sections. *C*, ×100 (*left*) and ×400 (*right*) images of H&E-stained lung sections obtained from mice infected with H37Rv, Rv-pptr-AB::PknB, and Rv-pptr-AB::PknA-B at 8 weeks postinfection. *G*, granuloma; *AS*, alveolar spaces; *FC*, foamy histiocytic cells.

in the activation loop of PknA to alanine has been reported to affect its autophosphorylation activity, with the T172A mutation having a more prominent effect (42). In addition to the activation loop, the activation region consists of a P+1 loop that is required for kinase-substrate interactions (Figs. 5*A* and 6*A*). To determine the roles of Thr^{172} and Thr^{174} of the activation loop and Thr^{180} of the P+1 loop in modulating the function of PknA in mycobacteria, we expressed and purified MBP-tagged PknA, $PknA_{T172A}$, $PknA_{T174A}$, $PknA_{TATA}$ (T172A,T174A), $PknA_{T180A}$, and $PknA_{T3A}$ (T172A,T174A,T180A triple mutant) and performed *in vitro* kinase assays using universal substrate myelin basic protein. Whereas $PknA_{TATA}$ retained ~30–50% activity compared with the wild type, PknA activity was completely abrogated in $PknA_{T172A}$, $PknA_{T180A}$, and $PknA_{T3A}$ mutants and partially abrogated in $PknA_{T174A}$ mutant (Fig. 7, *B–E*). The loss of activity of $PknA_{T180A}$ could either occur because Thr^{180} phosphorylation is critical for PknA function or be due to the loss of interactions mediated through the hydroxyl group on the threonine residue. To discriminate between the two possibilities, we mutated Thr^{180} to either a glutamate residue, which serves as a phosphomimetic amino acid, or to a serine residue, which can also provide a

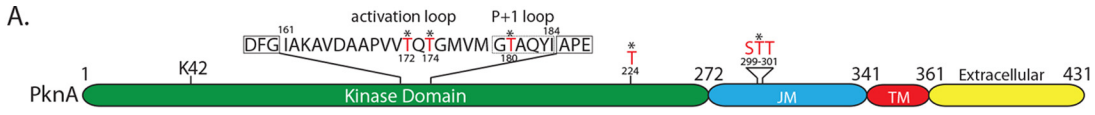

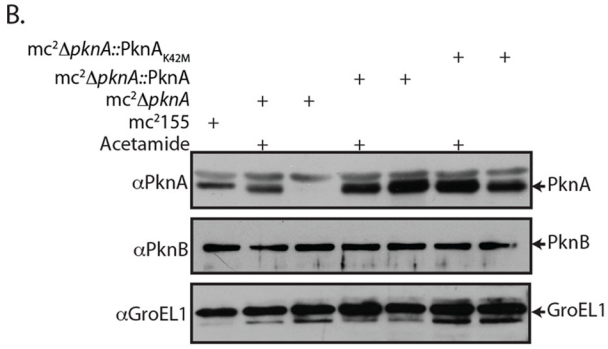

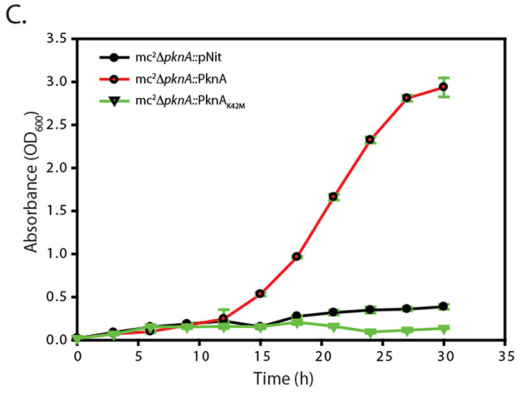

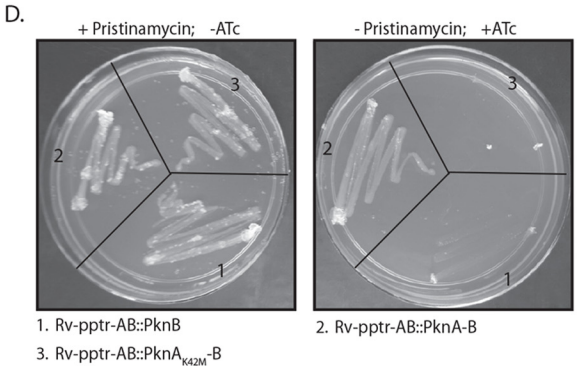

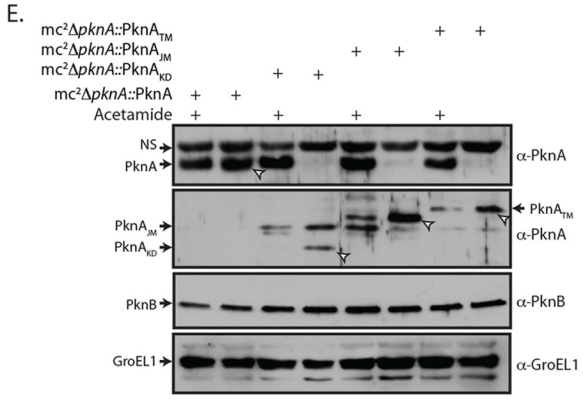

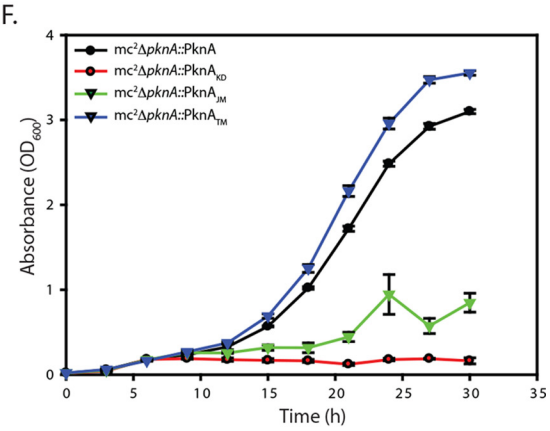

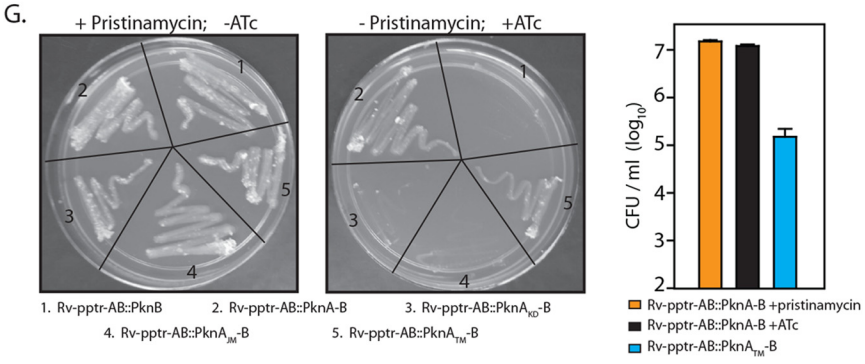

hydroxyl group. Whereas the $PknA_{T180E}$ mutant was inactive, the $PknA_{T180S}$ mutant partially restored activity (Fig. 7, *B* and *C*), implicating a role for the hydroxyl group of Thr^{180} in modulating PknA activity.

Phosphorylation of PknA on Its Activation Loop Is Crucial in Modulating Cell Growth—Next we examined the ability of $PknA_{TATA}$, $PknA_{T180A}$, and $PknA_{T3A}$ mutants to complement the deficit of wild type PknA in *M. tuberculosis*. The growth patterns on ATc plates (in the absence of wild type PknA) demonstrated that the $PknA_{T180A}$ and $PknA_{T3A}$ mutants could not functionally replace wild type PknA because there was no cell growth (Fig. 8*A*), in agreement with our findings that these two mutant proteins are unable to phosphorylate myelin basic protein (*MyBP*; Fig. 7, *B* and *C*). Although the $PknA_{TATA}$ mutant retained ~30–50% activity *in vitro* (Fig. 7, *B–E*), it was unable to completely rescue the PknA deficiency phenotype, with severely compromised growth on ATc plates (Fig. 8*A*), indicating the importance of activation loop phosphorylation for PknA function in mycobacteria. To investigate the importance of phosphorylation on either Thr^{172} or Thr^{174} or both residues concurrently, Rv-pptr-AB was transformed with pCiT-PknA-B rescue constructs containing either $PknA_{T172A}$-B, $PknA_{T174A}$-B, or $PknA_{TATA}$-B. The transformants were replica-streaked, and their growth patterns were observed. Although the $PknA_{T174A}$ mutant retained only 20% activity *in vitro* (Fig. 7, *D* and *E*), it behaved like the strain expressing wild type PknA. However, both $PknA_{T172A}$ and $PknA_{TATA}$ showed severely compromised growth (Fig. 8*B*). Western blot analysis indicated that the expression levels of PknA, $PknA_{T172A}$, $PknA_{T174A}$, $PknA_{TATA}$, or $PknA_{T180A}$ in the presence of ATc were comparable (Fig. 8*C*). We analyzed the viability of the Rv-pptr-AB strain complemented with the PknA-B or $PknA_{mutant}$-B constructs. Whereas the cfu obtained for $PknA_{T174A}$-expressing strain were similar to those obtained for PknA-expressing strain, both $PknA_{T172A}$- and $PknA_{TATA}$-expressing strains showed severely compromised viability (Fig. 8*D*). Taken together, these results suggest that phosphorylation of PknA at Thr^{172} of PknA is imperative for the survival of *M. tuberculosis*.

In addition to the activation loop, endogenous PknA has been shown to be phosphorylated at Thr^{224} in the kinase domain and on Ser^{229}, Thr^{300}, and Thr^{301} (STT) residues in the juxtamembrane domain (44) (Fig. 6*A*). To address any possible role these phosphorylations may play in modulating PknA function in mycobacteria, we mutated Thr^{224} to alanine, and STT residues (positions 299–301) were concurrently mutated to alanine residues (*M3* in Fig. 8). The complementation analyses showed that these phosphorylation events are dispensable for mycobacterial survival (Fig. 8*E*).

Activation of PknA through Loop Phosphorylation Is Independent of PknB—To examine the *in vivo* role of PknB in modulating the activation of PknA, we began by raising phospho-specific antibodies against a dually phosphorylated peptide whose sequence was derived from the activation loop sequence of PknA (Fig. 9*A*). The specificity of the antibodies was checked by expressing MBP-PknA, MBP-$PknA_{K42M}$, and MBP-$PknA_{TATA}$ in *E. coli* and probing them in Western blots with antibodies against PknA (α-PknA), phospho-Thr (α-Thr(P)), and PknA-$Thr(P)^{172}$,$Thr(P)^{174}$ (α-p-PknA). Although the wild type PknA could be detected with all three antibodies, kinase-inactive $PknA_{K42M}$ was detected with anti-PknA antibodies only, as expected, because this protein has lost the ability for autophosphorylation. The $PknA_{TATA}$ mutant was faintly detected with α-Thr(P) antibodies, signifying a substantial decrease in autophosphorylation activity following the absence of loop phosphorylation. Although the α-p-PknA antibodies recognized the wild type protein, they failed to recognize the $PknA_{TATA}$ mutant, establishing their specificity for detecting PknA phosphorylated at these specific residues in the activation loop (Fig. 9*B*). Although the phospho-specific antibodies were raised against dually phosphorylated peptide, we examined the possibility of them recognizing PknA phosphorylated either on Thr^{172} or on Thr^{174} residues. Probing with α-Thr(P) antibodies revealed that mutating either Thr^{172} or Thr^{174} residues in the activation loop had no impact on the autophosphorylation ability of PknA (Fig. 9*C*). Interestingly, the α-p-PknA antibodies robustly recognized PknA phosphorylated either on Thr^{172} or on Thr^{174} residues, indicating that the phospho-specific antibodies are capable of specifically recognizing phosphorylation at both residues individually (Fig. 9*C*). We then analyzed the ability of the α-p-PknA antibodies to recognize PknA expressed

FIGURE 6. **The extracellular domain of PknA is dispensable for cell survival.** *A*, schematic representation of PknA depicting activation segment sequence between the conserved DFG and APE motifs. Thr^{172} and Thr^{174} in the activation loop and Thr^{180} in the P+1 loop are indicated by an *asterisk*. Additional phosphorylation sites identified in the kinase domain and juxtamembrane regions (Thr^{224} and STT (residues 299–301)) are also indicated with *asterisks*. *B*, mc^2Δ*pknA* or mc^2Δ*pknA* transformed with pNit-PknA or pNit-$PknA_{K42M}$ were initially grown to an A_{600} of 0.8–1.0 in the presence of 0.5% acetamide. Fresh cultures were seeded at an initial A_{600} of 0.3, and the cultures were grown for 3 h in 7H9 medium. Cultures of mc^2Δ*pknA* were grown in the presence or absence of 0.5% acetamide. In the case of mc^2Δ*pknA* transformed with pNit-PknA or pNit-$PknA_{K42M}$, cultures were grown in the presence or absence of 0.5% acetamide or 0.2 μM IVN, as indicated. $mc^2$155 was grown in the absence of any inducer. WCLs were resolved and probed with α-PknA, α-PknB and α-GroEL1 antibodies. *C*, growth pattern analyses of *mc*^{2}Δ*pknA*::pNit or *mc*^{2}Δ*pknA*::PknA or *mc*^{2}Δ*pknA*::$PknA_{K42M}$ transformants grown in presence of 0.2 μM IVN, cultures were seeded at an initial A_{600} of 0.02. *Error bars*, S.E. *D*, midlog phase cultures of Rv-pptr-AB::PknB, Rv-pptr-AB::PknA-B, or Rv-pptr-AB::$PknA_{K42M}$-B were streaked on 7H10 agar plates containing either pristinamycin or ATc, as indicated. *E*, mc^2Δ*pknA* transformed with pNit-PknA, pNit-$PknA_{KD}$, pNit-$PknA_{JM}$, or pNit-$PknA_{TM}$ were initially grown to an A_{600} of 0.8–1.0 in the presence of 0.5% acetamide. Fresh cultures were seeded at an initial A_{600} of 0.3, and the cultures were grown for 3 h in 7H9 medium. In the case of mc^2Δ*pknA* transformed with pNit-PknA, pNit-$PknA_{KD}$, pNit-$PknA_{JM}$, or pNit-$PknA_{TM}$, cultures were grown in the presence or absence of 0.5% acetamide or 0.2 μM IVN as indicated. WCLs were resolved and probed with α-PknA, α-PknB, and α-GroEL1 antibodies. *White arrowheads* indicate PknA in *lane 2* and $PknA_{KD}$, $PknA_{JM}$, and $PknA_{TM}$ in *lanes 4*, *6*, and *8*, respectively. *F*, growth pattern analyses of mc^2Δ*pknA*::PknA or mc^2Δ*pknA*::$PknA_{KD}$ or mc^2Δ*pknA*::$PknA_{JM}$ or mc^2Δ*pknA*::$PknA_{TM}$ transformants grown in the presence of 0.2 μM IVN, cultures were seeded at an initial A_{600} of 0.02. *Error bars*, S.E. *G*, midlog phase cultures of Rv-pptr-AB::PknB, Rv-pptr-AB::PknA-B, Rv-pptr-AB::$PknA_{KD}$-B, Rv-pptr-AB::$PknA_{JM}$-B, Rv-pptr-AB::$PknA_{TM}$-B were diluted to A_{600} of 0.2, and 5 μl were streaked on 7H10 agar plates containing either pristinamycin or ATc. *H*, Rv-pptr-AB::PknA-B and Rv-pptr-AB::$PknA_{TM}$-B were initially grown to an A_{600} of 0.8 in presence of pristinamycin. Fresh cultures were seeded at an initial A_{600} of 0.1 and grown for 4 days. Rv-pptr-AB::PknA-B was grown in the presence of either pristinamycin or ATc, whereas Rv-pptr-AB::$PknA_{TM}$-B was grown in the presence of ATc only. After 4 days, cultures were serially diluted and plated on pristinamycin plates. cfu of Rv-pptr-AB::PknA-B grown in pristinamycin, Rv-pptr-AB::PknA-B grown in ATc, and Rv-pptr-AB::$PknA_{TM}$-B grown in ATc are 7.18 log_{10}, 7.08 log_{10}, and 5.18 log_{10}, respectively. Results were plotted with cfu log_{10} on the *y* axis, and samples are plotted on the *x* axis. The experiment was performed in triplicate, and the *error bars* represent S.D.

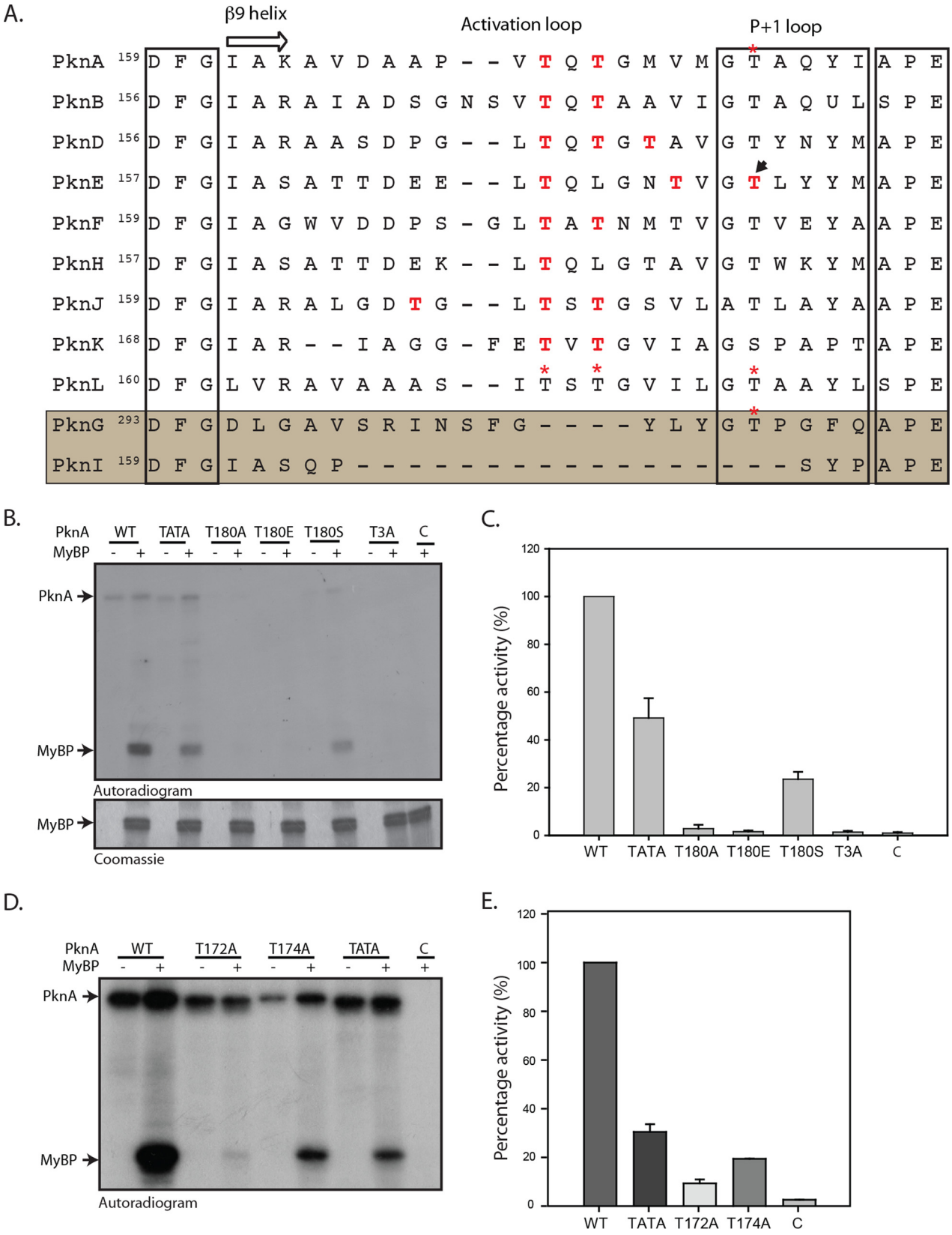

FIGURE 7. **Abrogation of phosphorylation in the activation segment affects catalytic activity of PknA.** *A*, multiple sequence alignment of the activation segment region of all 11 *M. tuberculosis* STPKs. Residues indicated with *red boldface type* are those identified as the target phosphorylation sites using mass spectrometry. The residue in the P+1 loop of PknE indicated with an *arrow* is identified with the help of mass spectrometry. PknG and PknI that do not contain the characteristic activation loop region have been *shaded*. *B* and *D*, *in vitro* kinase assays were performed in triplicates with 5 pmol of PknA or PknA mutants with or without 5 μg of myelin basic protein (*MyBP*) as the substrate. An autoradiogram is depicted in the *top panel*; the *bottom panel* in *B* shows Coomassie-stained myelin basic protein band. *C* and *E*, graphical representation of kinase activity of PknA mutants in *B* and *D*. Relative activity of the mutants is depicted with respect to PknA activity, which was fixed at 100%. *Error bars*, S.D.

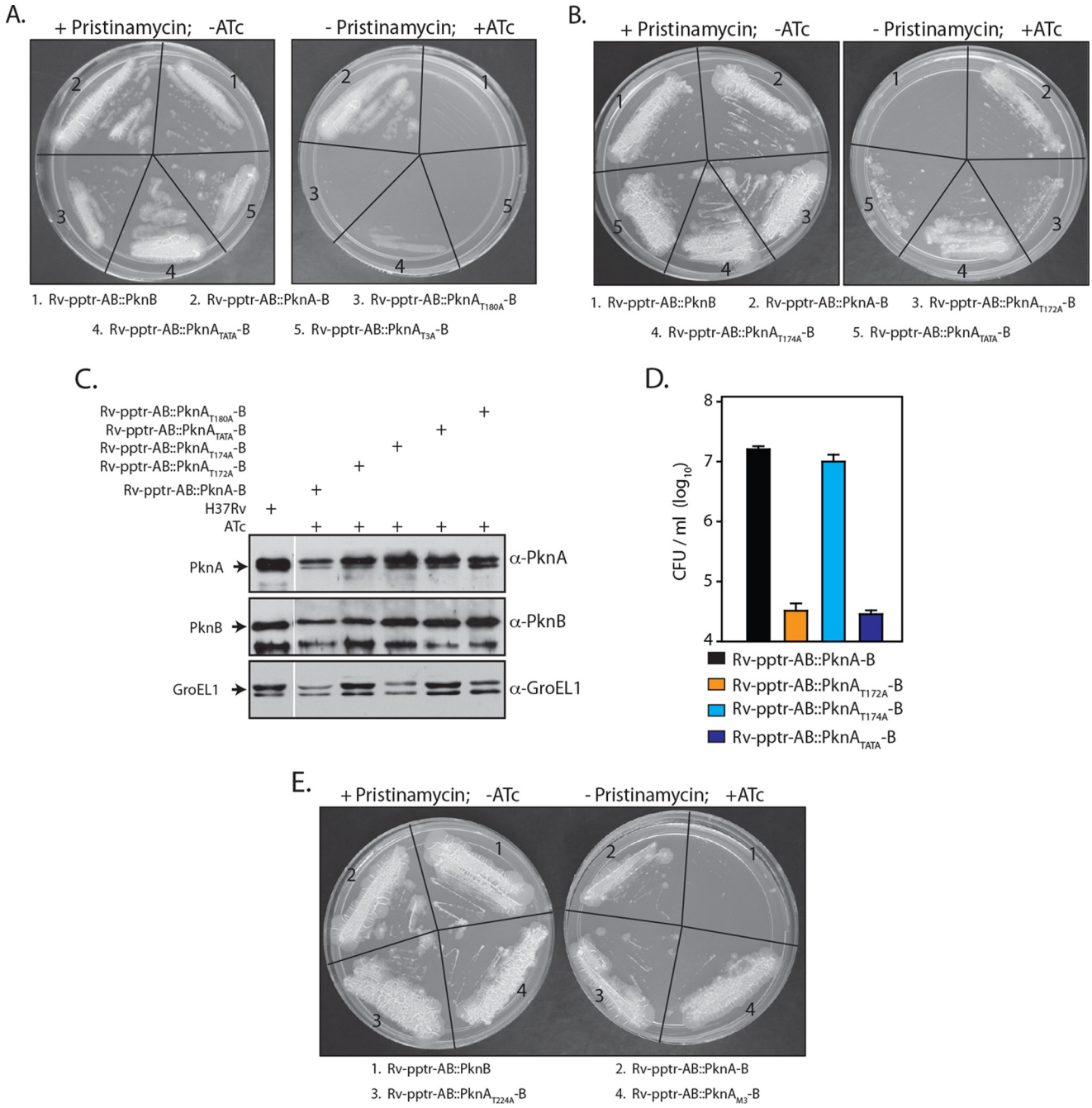

FIGURE 8. **Phosphorylation of PknA on its activation loop is crucial in modulating cell growth.** *A*, midlog phase cultures of Rv-pptr-AB::PknB, Rv-pptr-AB::PknA-B, Rv-pptr-AB::PknA$_{T180A}$-B, Rv-pptr-AB::PknA$_{TATA}$-B, or Rv-pptr-AB::PknA$_{T3A}$-B strains were streaked on 7H10 agar plates containing pristinamycin or ATc. *B*, midlog phase cultures of Rv-pptr-AB::PknB, Rv-pptr-AB::PknA-B, Rv-pptr-AB::PknA$_{T172A}$-B, Rv-pptr-AB::PknA$_{T174}$-B, or Rv-pptr-AB::PknA$_{TATA}$-B strains were streaked on 7H10 agar plates containing pristinamycin or ATc. *C*, cultures of H37Rv, Rv-pptr-AB::PknA-B, Rv-pptr-AB::PknA$_{T172A}$-B, Rv-pptr-AB::PknA$_{T174}$-B, Rv-pptr-AB::PknA$_{TATA}$-B, or Rv-pptr-AB::PknA$_{T180A}$-B were grown to an A_{600} of 0.8 in presence of pristinamcyin were used to seed fresh cultures at an initial A_{600} of 0.2. The cultures were grown in the presence of ATc as indicated for 4 days. H37Rv was grown in the absence of any inducer. WCLs were resolved and probed with α-PknA, α-PknB, α-GroEL1 antibodies. *D*, Rv-pptr-AB::PknA-B, Rv-pptr-AB::PknA$_{T172A}$-B, Rv-pptr-AB::PknA$_{T174}$-B, or Rv-pptr-AB::PknA$_{TATA}$-B were initially grown to an A_{600} of 0.8 in presence of pristinamycin. Fresh cultures were seeded at an initial A_{600} of 0.1 and grown for 4 days in the presence of ATc. After 4 days, cultures were serially diluted and plated on pristinamycin plates. Results were plotted with cfu $\log_{10}$ on the *y* axis and samples on the *x* axis. *Error bars*, S.E. *E*, midlog phase cultures of Rv-pptr-AB::PknB, Rv-pptr-AB::PknA-B, Rv-pptr-AB::PknA$_{T224A}$-B, or Rv-pptr-AB::PknA$_{M3}$-B strains were streaked on 7H10 agar plates containing pristinamycin or ATc.

in *M. smegmatis* by probing whole cell lysates isolated from mc^{2}Δ*pknA* transformed with either the pNit vector or pNit-PknA or pNit-PknA$_{mutant}$ constructs. PknA was verified to be robustly expressed in all of the transformed strains. However, although the wild type PknA was efficiently recognized by α-p-PknA antibodies, both PknA$_{K42M}$ and PknA$_{TATA}$ mutants could not be detected (Fig. 9*D*). The inability of these antibodies to detect PknA$_{TATA}$ protein was unsurprising because the target sites of phosphorylation, which would be recognized by the antibodies, are absent in this protein. However, the inability of the antibodies to detect PknA$_{K42M}$ was somewhat intriguing because it suggested that the activation loop, although amena-

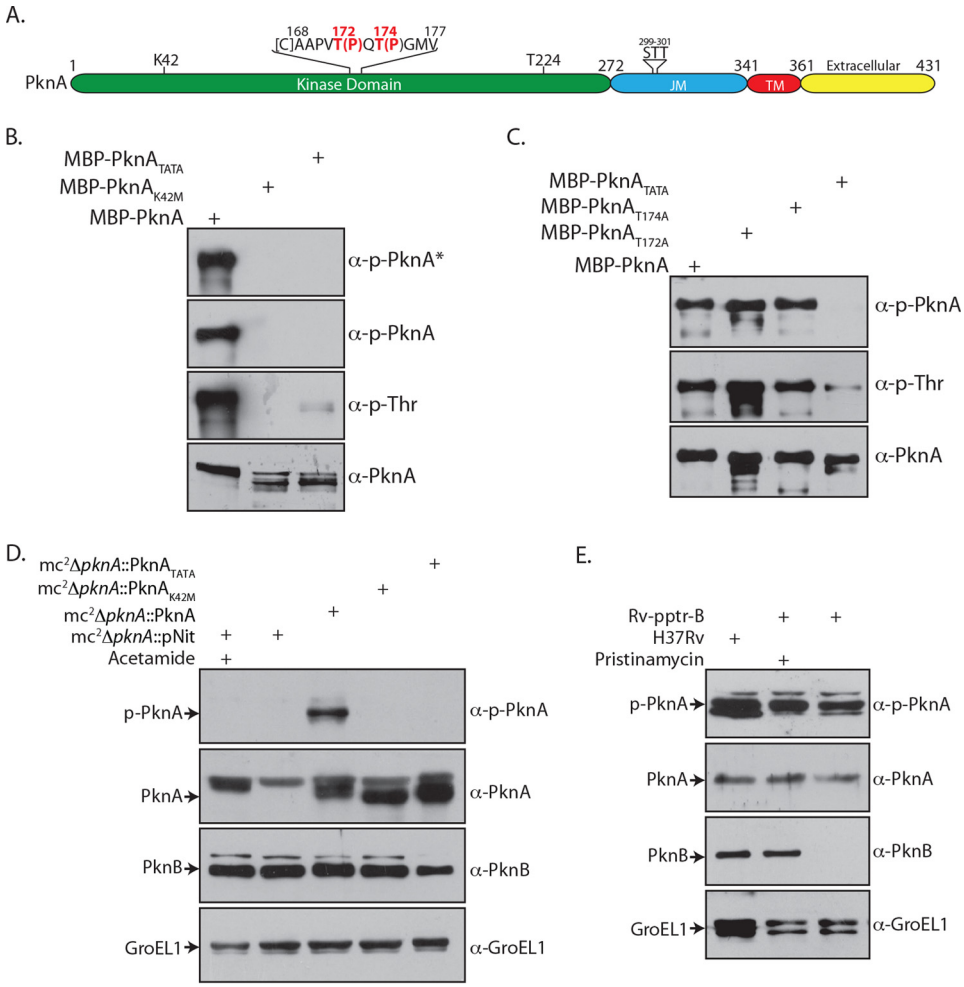

FIGURE 9. **Activation of PknA through loop phosphorylation is independent of PknB.** *A*, schematic depiction of PknA showing the dually phosphorylated phosphopeptide used for generation of phospho-specific antibodies. *B*, WCLs prepared from *E. coli* BL21 strain transformed with pMAL-PknA, pMAL-PknA$_{K42M}$, or pMAL-PknA$_{TATA}$ were resolved, transferred, and probed with α-PknA, α-Thr(P), and purified phospho-specific antibodies generated from two different rabbits, α-p-PknA* and α-p-PknA. α-p-PknA was selected for further work because of its higher sensitivity. *C*, WCLs prepared from *E. coli* BL21 strain transformed with pMAL-PknA, pMAL-PknA$_{T172A}$, pMAL-PknA$_{T174A}$, or pMAL-PknA$_{TATA}$ were resolved on SDS-PAGE, transferred onto nitrocellulose membrane, and probed with α-p-PknA, α-Thr(P), and α-PknA antibodies. *D*, mc^{2}Δ*pknA* transformed with pNit, pNit-PknA, pNit-PknA$_{K42M}$, or pNit-PknA$_{TATA}$ was grown to A_{600} of 0.8–1.0 in presence of acetamide 0.5%. Fresh cultures were seeded at an initial A_{600} of 0.3, and the cultures were grown for 5 h in 7H9 medium containing 0.2 μM IVN. In the case of mc^{2}Δ*pknA*::pNit, both IVN and acetamide were added to the culture medium. WCLs were resolved and probed with α-p-PknA, α-PknA, α-PknB, and α-GroEL1 antibodies. *E*, H37Rv and Rv-pptr-B cultures were seeded at an initial A_{600} of 0.2. WCLs prepared from H37Rv and Rv-pptr-B grown in the presence or absence of pristinamycin for 4 days were probed with α-p-PknA, α-PknA, α-PknB, and α-GroEL1 antibodies.

ble for *trans*-phosphorylation by regulatory kinase PknB (or other kinases), was in fact being activated only by autophosphorylation. This finding was further investigated by probing whole cell lysates isolated from H37Rv and Rv-pptr-B (strain in which transcription of the *pknB* gene is under the control of a pristinamycin-inducible promoter) (23) grown in the presence or absence of inducer (Fig. 9*E*). Although immunoblot analysis confirmed depletion of PknB in the absence of inducer, the endogenous PknA levels remained unaltered (Fig. 9*E*, compare *lane 3* with *lane 2*). Importantly, the activation loop phosphorylation of PknA remained unaltered despite PknB depletion (Fig. 9*E*). Thus, it appears that activation of PknA is most likely through autophosphorylation and is independent of PknB.

PknA and PknB Show Distinctive Patterns of Subcellular Localization—Catalytically inactive mVenus-PknA$_{D141N}$ has been shown to localize mostly to the midcell and the poles in previous studies (31), and the wild type RFP-PknB has been reported to localize to poles and midcell (40). However, the precise cellular localization of wild type PknA has not yet been deciphered. To investigate the precise subcellular localizations of PknA, *M. smegmatis* mc^{2}155 was transformed with pNit-mCherry-PknA or pMV306-RFP-PknB (40), and ~400–450 cells of each type were examined for direct fluorescence of the tagged proteins. In agreement with the previous report, a majority of the cells expressing RFP-PknB (82%) were localized to the poles and septum (40) (Fig. 10, *B*, *C*, and *G*). In addition, we also observed multisepta and distinct bipolar pattern (14%) and, less frequently, localization to membrane perimeter and poles. Contrary to PknB, the majority of the cells expressing mCherry-PknA (58%) displayed PknA expression at the membrane perimeter along the length of the cell (Fig. 10*E*), whereas a minor population showed PknA to localize at either or both poles (uni- and bipolar; 16 and 14%, respectively) and occasionally to both the poles and the midcell (12%) (Fig. 10, *E* and *F*). We determined the expression levels of RFP-PknB and mCherry-PknA relative to the wild type protein levels through

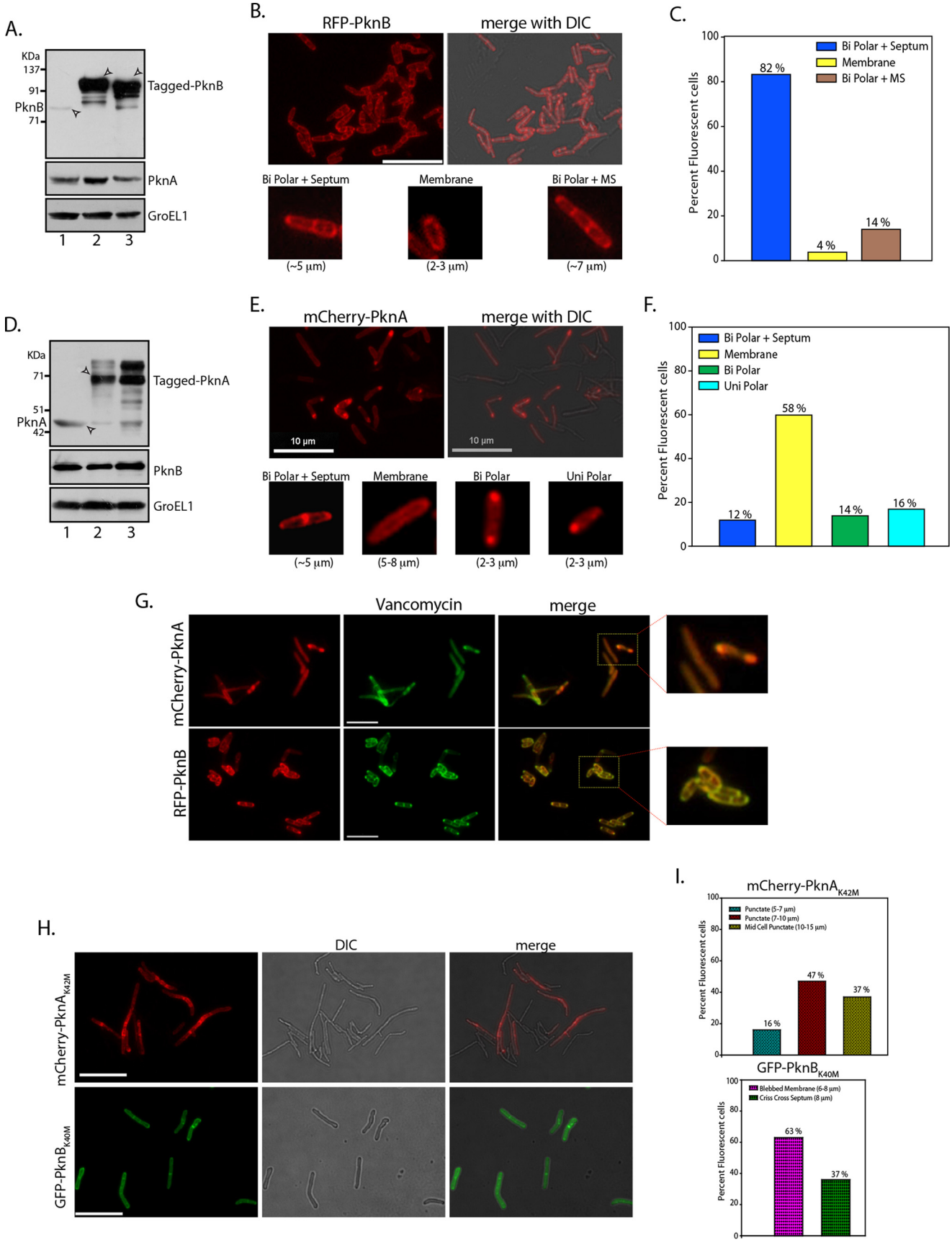

Western blots (Fig. 10, *A* and *D*). Whereas the expression levels of either RFP-PknB or GFP_m^{2+}-$PknB_{K40M}$ were found to be ~40-fold higher compared with endogenous PknB protein levels, the expression levels of mCherry-PknA or mCherry-$PknA_{K42M}$ were ~7-fold higher, relative to endogenous PknA protein levels (Fig. 10, *A* and *D*). These results indicate that the PknB almost always localizes to poles and septa, with a minor (4%) population showing only the pole localization. On the other hand, the localization of PknA also seems to be alternating between membrane perimeter or at the poles, with the majority of cells showing membrane perimeter localization. Our efforts to co-express both GFP-PknA and RFP-PknB to investigate the localization of PknA and PknB in the same cell were unsuccessful, most likely because overexpression of both PknA and PknB together in the cell is detrimental to bacterial survival.

We next investigated the co-localization of mCherry-PknA or RFP-PknB with vancomycin-FL (Van-FL), a fluorescein-tagged antibiotic that binds with nascent peptidoglycans and marks the sites of active cell growth. In RFP-PknB-expressing cells, Van-FL showed consistent staining at cell poles and septum, and RFP-PknB co-localized with Van-FL (Fig. 10*G*, *bottom*). However, the Van-FL labeling varied from one cell to the other in mCherry-PknA-expressing cells. In cells where mCherry-PknA localized to either poles or mid cell, we observed co-localization with Van-FL staining (Fig. 10*G*, *top*). Interestingly, in the cells showing mCherry-PknA along the cell membrane, the Van-FL staining seems to have been dispersed throughout the cell (Fig. 10*G*). Thus, overexpression of PknA (mCherry-PknA) or PknB (RFP-PknB) seems to differentially impact the sites of active cell growth.

Expression of catalytically inactive StkP in *Streptococcus pneumoniae* significantly altered the morphology of the organism, converting it from diplococcic to elongated, rod-shaped cells (45). Because both PknA and PknB are independently essential for cell growth and survival, we examined whether the overexpression of kinase-inactive mutants would influence cell morphology. Cells expressing mCherry-$PknA_{K42M}$ appeared to be significantly elongated, with $PknA_{K42M}$ localized mostly to the midcell with fluorescence intensities gradually tapering toward the poles (Fig. 10, *H* and *I*, *top panels*). Although expression of GFP_m^{2+}-$PknB_{K40M}$ did not alter cell length significantly, it caused severe aberrations in cell shape with blebs at the poles (Fig. 10, *H* and *I*, *bottom panels*). Furthermore, the localization of kinase-inactive mutant ($PknB_{K40M}$) was mostly observed along the membrane, and the characteristic pole and septum localization pattern observed with the wild type PknB could not be detected. Taken together, these experiments suggest that PknA and PknB are likely to be engaging cell wall synthesis and cell division machinery in distinctive ways.

DISCUSSION

Gene replacement mutants are powerful tools used to investigate the role of a gene in modulating cellular function. Although gene deletion or transposon mutants of 8 of the 11 STPKs of *M. tuberculosis* have been utilized to assess their functions (24, 46–52), the impact of disrupting the genes encoding the kinases PknL, PknF, and PknA has yet to be reported. In the present study, we have evaluated the role of PknA in modulating *in vitro* growth and survival of the pathogen in its host. Although we were successful in creating a Δ*pknA* mutant of *M. smegmatis*, obtaining a Δ*pknA* mutant of *M. tuberculosis* was challenging due to the fact that *pknA* lies upstream of *pknB.* Therefore, we adopted the route of first creating a conditional double mutant, Rv-pptr-AB, and then modifying this strain by providing an additional copy of *pknB* to create a *pknA* conditional mutant. We have previously shown that the depletion of PknB causes a bactericidal phenotype with an ~3 log-fold decrease in survival (24). Here we observe that the depletion of PknA results in an ~4 log-fold decrease in survival (Fig. 3). Interestingly, depletion of both PknA and PknB seems to have a cumulative negative bearing on growth of the pathogen (Fig. 3).

The overexpression or depletion of several STPKs has been shown to impact cellular morphology. For example, the overexpression of PknF in *M. smegmatis* led to the shortening of bacilli, and reduced expression of PknF in *M. tuberculosis* led to reduced growth and deformed morphology (53), and analysis of the morphology of the *M. tuberculosis pknK* deletion mutant by scanning electron microscopy also shows deviant morphology with unusually shortened cells (47). We have previously shown that the overexpression or depletion of the essential kinase PknB in *M. smegmatis* results in shrinkage of cells and subsequent cell lysis (24). The overexpression of PknA in *Mycobacterium bovis* BCG has been shown to result in aberrant cell morphology, with the cells forming an elongated and branched structure (19). We observe that depletion of PknA in *M. tuberculosis* results in elongated cells, and prolonged depletion results in fused cells on the verge of lysis (Fig. 3). Importantly, concurrent depletion of both PknA and PknB severely impacts

FIGURE 10. **Cellular localization of PknA and PknB shows distinct pattern.** *A*, fresh cultures of mc^2155 or mc^2155::RFP-PknB or mc^2155::GFP_m^{2+}-$PknB_{K40M}$ were grown in fresh 7H9 medium until an A_{600} of 0.8–1.0 in the presence of appropriate inducers as described under "Materials and Methods." WCLs were probed with α-PknA, α-PknB, and α-GroEL1 antibodies. *Top*, *white arrowhead* in *lane 1* indicates endogenous PknB; *white arrowhead* in *lanes 2* and *3* indicate RFP-PknB and GFP_m^{2+}-$PknB_{K40M}$, respectively. *B*, fluorescence and differential interference contrast images of *M. smegmatis* transformed with RFP-PknB; *scale bar*, 10 μm. *Bottom*, *enlarged images* of RFP-PknB with different localization patterns. *C*, quantification of different RFP-PknB localization patterns ($n = 404$) from three independent experiments. *D*, fresh cultures of mc^2155 or mc^2155::mCherry-PknA or mc^2155::mCherry-$PknA_{K42M}$ were grown in fresh 7H9 medium until an A_{600} of 0.8–1.0 in the presence of appropriate inducers as described under "Materials and Methods." WCLs were probed with α-PknA, α-PknB, and α-GroEL1 antibodies. *Top*, *white arrowhead* in *lane 1* indicates endogenous PknA; *white arrowheads* in *lanes 2* and *3* indicate mCherry-PknA and mCherry-$PknA_{K42M}$, respectively. *E*, fluorescence and differential interference contrast images of *M. smegmatis* transformed with mCherry-PknA; *scale bar*, 10 μm. *Bottom*, *enlarged images* of mCherry-PknA with different localization patterns. *F*, quantification of different mCherry-PknA localization patterns ($n = 440$) from three independent experiments. *G*, fluorescence analysis of *M. smegmatis* expressing either mCherry-PknA or RFP-PknB incubated with Van-FL as described under "Materials and Methods"; *scale bar*, 10 μm. *Top*, *inset* shows *enlarged images* of Van-FL co-localization with mCherry-PknA. *Bottom*, *inset* shows *enlarged images* of Van-FL co-localization with RFP-PknB. *H*, fluorescence, differential interference contrast, and merge images of *M. smegmatis* expressing mCherry-$PknA_{K42M}$ or GFP_m^{2+}-$PknB_{K40M}$; *scale bar*, 10 μm. *I*, quantification of fluorescent cells showing aberrant cell morphologies. *Top*, results for mCherry-$PknA_{K42M}$-expressing cells ($n = 325$) from three independent experiments. *Bottom*, data for GFP_m^{2+}-$PknB_{K40M}$-expressing cells ($n = 325$) from three independent experiments.

the cell morphology (Fig. 3). Results from studies carried out by infecting mice with the pathogen establish for the first time that PknA is indispensable for the bacterium to establish infection and for persistent survival of *M. tuberculosis* in the host (Fig. 4). This is corroborated by the observed reduction in histological damage in the absence of PknA (Fig. 5).

The domain architecture of the mycobacterial STPKs is broadly conserved. Nine of the 11 STPKs contain intracellular N-terminal kinase and juxtamembrane domains followed by a single helix transmembrane domain and an extracytoplasmic domain of varied length (15). The domain organization of PknG is unique because it contains an N-terminal rubredoxin domain, which is essential for its activity (54), and PknK (the largest kinase) also requires the C-terminal region for efficient activity in addition to its kinase domain (55). With the exception of PknA, the kinase domains of the remaining transmembrane domain-containing STPKs have the ability to carry out phosphorylations independent of the presence of the other domains (27). The kinase domain along with the juxtamembrane region of PknA is absolutely essential for its activity *in vitro* (31, 42). In concurrence with these findings, the $PknA_{KD}$ protein is unable to rescue the PknA depletion phenotype (Fig. 6). Additionally, $PknA_{JM}$ (which contains the juxtamembrane domain as well) also fails to complement the PknA function. Interestingly, $PknA_{TM}$, which contains the putative transmembrane domain but not the extracytoplasmic domain, can complement PknA function (Fig. 6). Thus, the extracytoplasmic domain of PknA seems to be dispensable for PknA function (Fig. 6).

Phosphorylations of the activation loop of protein kinases alter their conformation and stabilize the intramolecular interactions in the kinase domain, thus enhancing their catalytic activity (43). Alignment of the amino acid sequences of the *M. tuberculosis* STPKs has revealed the activation segment to contain one or more conserved threonine residues (exceptions being PknG and PknI; Fig. 7*A*) (56). With the help of mass spectrometry analysis, the autophosphorylation sites in the activation loop have been identified in PknA, PknB, PknD, PknE, PknH, and PknF (56, 57). Whereas *in vitro* kinase assays with wild type and active site mutant proteins have established the critical activation loop residues in the cases of PknK and PknJ (55, 58), the activation of PknG has been found to be independent of activation loop phosphorylations (54, 59). *In vitro* kinase assays with PknA have shown the activation of PknA to be regulated through the phosphorylation of threonine residues in the activation segment (42, 57). Although both Thr^{172} and Thr^{174} in the activation loop of PknA have been shown to be autophosphorylated, we find that mutating these residues decreases the activity of PknA by 30–50% (Fig. 7). However, complementation experiments demonstrate that the phosphorylation of the Thr^{172} residue of PknA is crucial for its function in *M. tuberculosis* (Fig. 8). In addition to the conserved threonine residues in the activation loop, a threonine in the P+1 loop has also been identified to be autophosphorylated in PknE (56) (indicated in Fig. 7*A*). Our findings indicate that the hydroxyl group of threonine in the P+1 loop of PknA (Thr^{180}) is critical for activity of the protein. Prisic *et al.* (44) have identified phosphorylation sites in the kinase domain and juxtamembrane domain of endogenous PknA. We find that mutating the identified sites does not have any influence on complementation of PknA function (Fig. 8). Although these phosphorylation events may not be crucial for PknA-mediated cell survival, we cannot rule out the possibility of these sites being involved in modulating protein-protein interactions or the activity of PknA.

In eukaryotes, the concept of signaling cascades wherein the signal is transduced from the environment to a kinase, and from one kinase to the next in the chain through phosphorylations of the activation loop residues, is very well established. Although there are 11 protein kinases in *M. tuberculosis*, the presence of such signaling cascades has not yet been established. Recently, in an elegant and systematic study (31), PknB and PknH have been proposed to be the master regulators that modulate the activation of substrate kinases. The extracytoplasmic PASTA domains of PknB are required for its localization to the cell poles and septum and have the ability to interact with muropeptides (40). We have previously shown that the extracellular PASTA domains are necessary for PknB function in mycobacteria (24). Further, the protein levels of PknB are down-regulated under hypoxic conditions (60). Taken together, PknB is speculated to be the sensor kinase capable of responding to signals in the extracellular milieu, which in turn would activate other cellular kinases, including PknA, through activation loop phosphorylations (19, 31, 40). The fact that both PknA and PknB modulate similar processes such as cell division and cell wall synthesis lends credence to this hypothesis. Alternatively, the activation of PknA could be independent of PknB, with both of the kinases regulating similar cellular processes by modulating functions of different target proteins. To delineate between these two possibilities, we have raised and characterized phospho-specific antibodies capable of specifically recognizing the activation loop phosphorylation(s) of PknA (Fig. 9). Data obtained using $mc^2\Delta pknA$ transformants suggest that the activation of PknA is through autophosphorylation (Fig. 9). Most importantly, depletion of PknB in *M. tuberculosis* did not alter the levels of PknA loop phosphorylation (Fig. 9).

Western blot analysis of subcellular fractions shows that whereas PknB predominantly localizes to the cell wall fraction, PknA localizes equally to both cell membrane and cell wall fractions (40). We observe that the localization of wild type PknA and PknB in mycobacteria appears to be distinctive, with a majority of PknA being localized along the cell perimeter and most of the PknB localizing to the poles and septum (Fig. 10). Based on these data, we suggest that the activation of PknA is independent of PknB. However, we cannot rule out cross-talk between PknA- and PknB-mediated signaling. Protein kinase StkP is shown to regulate cell shape and division in *S. pneumoniae*, and its interaction with GpsB protein is required to regulate its autophosphorylation (61). Complementing *S. pneumoniae* Δ*stkp* mutant with inactive StkP altered the cell morphology, converting it from diplococcic to elongated rod-shaped cells (45). Results presented in Fig. 10 show that overexpressing inactive PknA predominantly affects cell length, whereas the expression of the inactive PknB mutant protein causes the cell to bleb at the poles (Fig. 10). Moreover, the nature of vancomycin FL staining on cells overexpressing PknA or PknB seems to be distinctive (Fig. 10). Based on these results, our study suggests that,

although PknA and PknB are encoded from the same operon, their mode of activation and regulation of cellular processes seems to be independent of each other.

Acknowledgments—We acknowledge Dr. Rajmani for help with animal infection experiments. We thank Rekha Rani (National Institute of Immunology) for support in obtaining scanning electron microscopy images. We thank the Tuberculosis Aerosol Challenge Facility, International Centre for Genetic Engineering and Biotechnology (ICGEB) (New Delhi, India) for providing the facility to perform animal infection experiments. We thank Dr. Christopher M. Sassetti, Dr. Tanya Parish, Dr. Anil K. Tyagi, and Dr. Stewart Cole for providing the reagents.

REFERENCES

1. Graves, J. D., and Krebs, E. G. (1999) Protein phosphorylation and signal transduction. *Pharmacol. Ther.* **82,** 111–121
2. Spange, S., Wagner, T., Heinzel, T., and Krämer, O. H. (2009) Acetylation of non-histone proteins modulates cellular signalling at multiple levels. *Int. J. Biochem. Cell Biol.* **41,** 185–198
3. Hershko, A. (1983) Ubiquitin: roles in protein modification and breakdown. *Cell* **34,** 11–12
4. Stock, J. B., Ninfa, A. J., and Stock, A. M. (1989) Protein phosphorylation and regulation of adaptive responses in bacteria. *Microbiol. Rev.* **53,** 450–490
5. Whitmarsh, A. J., and Davis, R. J. (2000) Regulation of transcription factor function by phosphorylation. *Cell. Mol. Life Sci.* **57,** 1172–1183
6. Dorée, M., and Galas, S. (1994) The cyclin-dependent protein kinases and the control of cell division. *FASEB J.* **8,** 1114–1121
7. Hanks, S. K., and Hunter, T. (1995) Protein kinases 6. The eukaryotic protein kinase superfamily: kinase (catalytic) domain structure and classification. *FASEB J.* **9,** 576–596
8. Bakal, C. J., and Davies, J. E. (2000) No longer an exclusive club: eukaryotic signalling domains in bacteria. *Trends Cell Biol.* **10,** 32–38
9. Stock, A. M., Robinson, V. L., and Goudreau, P. N. (2000) Two-component signal transduction. *Annu. Rev. Biochem.* **69,** 183–215
10. Grangeasse, C., Nessler, S., and Mijakovic, I. (2012) Bacterial tyrosine kinases: evolution, biological function and structural insights. *Philos. Trans. R. Soc. Lond. B Biol. Sci.* **367,** 2640–2655
11. Petranovic, D., Michelsen, O., Zahradka, K., Silva, C., Petranovic, M., Jensen, P. R., and Mijakovic, I. (2007) *Bacillus subtilis* strain deficient for the protein-tyrosine kinase PtkA exhibits impaired DNA replication. *Mol. Microbiol.* **63,** 1797–1805
12. Ferreira, A. S., Silva, I. N., Oliveira, V. H., Becker, J. D., Givskov, M., Ryan, R. P., Fernandes, F., and Moreira, L. M. (2013) Comparative transcriptomic analysis of the *Burkholderia cepacia* tyrosine kinase bceF mutant reveals a role in tolerance to stress, biofilm formation, and virulence. *Appl. Environ. Microbiol.* **79,** 3009–3020
13. Lacour, S., Doublet, P., Obadia, B., Cozzone, A. J., and Grangeasse, C. (2006) A novel role for protein-tyrosine kinase Etk from *Escherichia coli* K-12 related to polymyxin resistance. *Res. Microbiol.* **157,** 637–641
14. Bach, H., Wong, D., and Av-Gay, Y. (2009) *Mycobacterium tuberculosis* PtkA is a novel protein tyrosine kinase whose substrate is PtpA. *Biochem. J.* **420,** 155–160
15. Av-Gay, Y., and Everett, M. (2000) The eukaryotic-like Ser/Thr protein kinases of *Mycobacterium tuberculosis*. *Trends Microbiol.* **8,** 238–244
16. Wiley, D. J., Nordfeldth, R., Rosenzweig, J., DaFonseca, C. J., Gustin, R., Wolf-Watz, H., and Schesser, K. (2006) The Ser/Thr kinase activity of the *Yersinia* protein kinase A (YpkA) is necessary for full virulence in the mouse, mollifying phagocytes, and disrupting the eukaryotic cytoskeleton. *Microb. Pathog.* **40,** 234–243
17. Sasková, L., Nováková, L., Basler, M., and Branny, P. (2007) Eukaryotic-type serine/threonine protein kinase StkP is a global regulator of gene expression in *Streptococcus pneumoniae*. *J. Bacteriol.* **189,** 4168–4179
18. Pereira, S. F., Goss, L., and Dworkin, J. (2011) Eukaryote-like serine/threonine kinases and phosphatases in bacteria. *Microbiol. Mol. Biol. Rev.* **75,** 192–212
19. Kang, C. M., Abbott, D. W., Park, S. T., Dascher, C. C., Cantley, L. C., and Husson, R. N. (2005) The *Mycobacterium tuberculosis* serine/threonine kinases PknA and PknB: substrate identification and regulation of cell shape. *Genes Dev.* **19,** 1692–1704
20. Chaba, R., Raje, M., and Chakraborti, P. K. (2002) Evidence that a eukaryotic-type serine/threonine protein kinase from *Mycobacterium tuberculosis* regulates morphological changes associated with cell division. *Eur. J. Biochem.* **269,** 1078–1085
21. Chakraborti, P. K., Matange, N., Nandicoori, V. K., Singh, Y., Tyagi, J. S., and Visweswariah, S. S. (2011) Signalling mechanisms in *Mycobacteria*. *Tuberculosis* **91,** 432–440
22. Sassetti, C. M., Boyd, D. H., and Rubin, E. J. (2003) Genes required for mycobacterial growth defined by high density mutagenesis. *Mol. Microbiol.* **48,** 77–84
23. Forti, F., Crosta, A., and Ghisotti, D. (2009) Pristinamycin-inducible gene regulation in mycobacteria. *J. Biotechnol.* **140,** 270–277
24. Chawla, Y., Upadhyay, S., Khan, S., Nagarajan, S. N., Forti, F., and Nandicoori, V. K. (2014) Protein kinase B (PknB) of *Mycobacterium tuberculosis* is essential for growth of the pathogen *in vitro* as well as for survival within the host. *J. Biol. Chem.* **289,** 13858–13875
25. Thakur, M., and Chakraborti, P. K. (2006) GTPase activity of mycobacterial FtsZ is impaired due to its transphosphorylation by the eukaryotic-type Ser/Thr kinase, PknA. *J. Biol. Chem.* **281,** 40107–40113
26. Dasgupta, A., Datta, P., Kundu, M., and Basu, J. (2006) The serine/threonine kinase PknB of *Mycobacterium tuberculosis* phosphorylates PBPA, a penicillin-binding protein required for cell division. *Microbiology* **152,** 493–504
27. Khan, S., Nagarajan, S. N., Parikh, A., Samantaray, S., Singh, A., Kumar, D., Roy, R. P., Bhatt, A., and Nandicoori, V. K. (2010) Phosphorylation of enoyl-acyl carrier protein reductase InhA impacts mycobacterial growth and survival. *J. Biol. Chem.* **285,** 37860–37871
28. Molle, V., and Kremer, L. (2010) Division and cell envelope regulation by Ser/Thr phosphorylation: *Mycobacterium* shows the way. *Mol. Microbiol.* **75,** 1064–1077
29. Sharma, K., Gupta, M., Krupa, A., Srinivasan, N., and Singh, Y. (2006) EmbR, a regulatory protein with ATPase activity, is a substrate of multiple serine/threonine kinases and phosphatase in *Mycobacterium tuberculosis*. *FEBS J.* **273,** 2711–2721
30. Molle, V., Brown, A. K., Besra, G. S., Cozzone, A. J., and Kremer, L. (2006) The condensing activities of the *Mycobacterium tuberculosis* type II fatty acid synthase are differentially regulated by phosphorylation. *J. Biol. Chem.* **281,** 30094–30103
31. Baer, C. E., Iavarone, A. T., Alber, T., and Sassetti, C. M. (2014) Biochemical and spatial coincidence in the provisional Ser/Thr protein kinase interaction network of *Mycobacterium tuberculosis*. *J. Biol. Chem.* **289,** 20422–20433
32. Parikh, A., Kumar, D., Chawla, Y., Kurthkoti, K., Khan, S., Varshney, U., and Nandicoori, V. K. (2013) Development of a new generation of vectors for gene expression, gene replacement, and protein-protein interaction studies in mycobacteria. *Appl. Environ. Microbiol.* **79,** 1718–1729
33. Pandey, A. K., Raman, S., Proff, R., Joshi, S., Kang, C. M., Rubin, E. J., Husson, R. N., and Sassetti, C. M. (2009) Nitrile-inducible gene expression in mycobacteria. *Tuberculosis* **89,** 12–16
34. Triccas, J. A., Parish, T., Britton, W. J., and Gicquel, B. (1998) An inducible expression system permitting the efficient purification of a recombinant antigen from *Mycobacterium smegmatis*. *FEMS Microbiol. Lett.* **167,** 151–156
35. Reddy, P. V., Puri, R. V., Chauhan, P., Kar, R., Rohilla, A., Khera, A., and Tyagi, A. K. (2013) Disruption of mycobactin biosynthesis leads to attenuation of *Mycobacterium tuberculosis* for growth and virulence. *J. Infect. Dis.* **208,** 1255–1265
36. Parish, T., and Stoker, N. G. (2000) Use of a flexible cassette method to generate a double unmarked *Mycobacterium tuberculosis* tlyA plcABC mutant by gene replacement. *Microbiology* **146,** 1969–1975
37. Carroll, P., Schreuder, L. J., Muwanguzi-Karugaba, J., Wiles, S., Robertson, B. D., Ripoll, J., Ward, T. H., Bancroft, G. J., Schaible, U. E., and Parish, T. (2010) Sensitive detection of gene expression in mycobacteria under rep-

licating and non-replicating conditions using optimized far-red reporters. *PLoS One* **5,** e9823
38. Song, H., Sandie, R., Wang, Y., Andrade-Navarro, M. A., and Niederweis, M. (2008) Identification of outer membrane proteins of *Mycobacterium tuberculosis*. *Tuberculosis* **88,** 526–544
39. Parikh, A., Verma, S. K., Khan, S., Prakash, B., and Nandicoori, V. K. (2009) PknB-mediated phosphorylation of a novel substrate, *N*-acetylglucosamine-1-phosphate uridyltransferase, modulates its acetyltransferase activity. *J. Mol. Biol.* **386,** 451–464
40. Mir, M., Asong, J., Li, X., Cardot, J., Boons, G. J., and Husson, R. N. (2011) The extracytoplasmic domain of the *Mycobacterium tuberculosis* Ser/Thr kinase PknB binds specific muropeptides and is required for PknB localization. *PLoS Pathog.* **7,** e1002182
41. Kang, C. M., Nyayapathy, S., Lee, J. Y., Suh, J. W., and Husson, R. N. (2008) Wag31, a homologue of the cell division protein DivIVA, regulates growth, morphology and polar cell wall synthesis in mycobacteria. *Microbiology* **154,** 725–735
42. Thakur, M., Chaba, R., Mondal, A. K., and Chakraborti, P. K. (2008) Interdomain interaction reconstitutes the functionality of PknA, a eukaryotic type Ser/Thr kinase from *Mycobacterium tuberculosis*. *J. Biol. Chem.* **283,** 8023–8033
43. Nolen, B., Taylor, S., and Ghosh, G. (2004) Regulation of protein kinases; controlling activity through activation segment conformation. *Mol. Cell* **15,** 661–675
44. Prisic, S., Dankwa, S., Schwartz, D., Chou, M. F., Locasale, J. W., Kang, C. M., Bemis, G., Church, G. M., Steen, H., and Husson, R. N. (2010) Extensive phosphorylation with overlapping specificity by *Mycobacterium tuberculosis* serine/threonine protein kinases. *Proc. Natl. Acad. Sci. U.S.A.* **107,** 7521–7526
45. Fleurie, A., Cluzel, C., Guiral, S., Freton, C., Galisson, F., Zanella-Cleon, I., Di Guilmi, A. M., and Grangeasse, C. (2012) Mutational dissection of the S/T-kinase StkP reveals crucial roles in cell division of *Streptococcus pneumoniae*. *Mol. Microbiol.* **83,** 746–758
46. Be, N. A., Bishai, W. R., and Jain, S. K. (2012) Role of *Mycobacterium tuberculosis* pknD in the pathogenesis of central nervous system tuberculosis. *BMC Microbiol.* **12,** 7
47. Malhotra, V., Arteaga-Cortés, L. T., Clay, G., and Clark-Curtiss, J. E. (2010) *Mycobacterium tuberculosis* protein kinase K confers survival advantage during early infection in mice and regulates growth in culture and during persistent infection: implications in immune modulation. *Microbiology* **156,** 2829–2841
48. Cowley, S., Ko, M., Pick, N., Chow, R., Downing, K. J., Gordhan, B. G., Betts, J. C., Mizrahi, V., Smith, D. A., Stokes, R. W., and Av-Gay, Y. (2004) The *Mycobacterium tuberculosis* protein serine/threonine kinase PknG is linked to cellular glutamate/glutamine levels and is important for growth *in vivo*. *Mol. Microbiol.* **52,** 1691–1702
49. Papavinasasundaram, K. G., Chan, B., Chung, J. H., Colston, M. J., Davis, E. O., and Av-Gay, Y. (2005) Deletion of the *Mycobacterium tuberculosis* pknH gene confers a higher bacillary load during the chronic phase of infection in BALB/c mice. *J. Bacteriol.* **187,** 5751–5760
50. Jayakumar, D., Jacobs, W. R., Jr., and Narayanan, S. (2008) Protein kinase E of *Mycobacterium tuberculosis* has a role in the nitric oxide stress response and apoptosis in a human macrophage model of infection. *Cell Microbiol.* **10,** 365–374
51. Gopalaswamy, R., Narayanan, S., Chen, B., Jacobs, W. R., and Av-Gay, Y. (2009) The serine/threonine protein kinase PknI controls the growth of *Mycobacterium tuberculosis* upon infection. *FEMS Microbiol. Lett.* **295,** 23–29
52. Jang, J., Stella, A., Boudou, F., Levillain, F., Darthuy, E., Vaubourgeix, J., Wang, C., Bardou, F., Puzo, G., Gilleron, M., Burlet-Schiltz, O., Monsarrat, B., Brodin, P., Gicquel, B., and Neyrolles, O. (2010) Functional characterization of the *Mycobacterium tuberculosis* serine/threonine kinase PknJ. *Microbiology* **156,** 1619–1631
53. Deol, P., Vohra, R., Saini, A. K., Singh, A., Chandra, H., Chopra, P., Das, T. K., Tyagi, A. K., and Singh, Y. (2005) Role of *Mycobacterium tuberculosis* Ser/Thr kinase PknF: implications in glucose transport and cell division. *J. Bacteriol.* **187,** 3415–3420
54. Tiwari, D., Singh, R. K., Goswami, K., Verma, S. K., Prakash, B., and Nandicoori, V. K. (2009) Key residues in *Mycobacterium tuberculosis* protein kinase G play a role in regulating kinase activity and survival in the host. *J. Biol. Chem.* **284,** 27467–27479
55. Kumar, P., Kumar, D., Parikh, A., Rananaware, D., Gupta, M., Singh, Y., and Nandicoori, V. K. (2009) The *Mycobacterium tuberculosis* protein kinase K modulates activation of transcription from the promoter of mycobacterial monooxygenase operon through phosphorylation of the transcriptional regulator VirS. *J. Biol. Chem.* **284,** 11090–11099
56. Durán, R., Villarino, A., Bellinzoni, M., Wehenkel, A., Fernandez, P., Boitel, B., Cole, S. T., Alzari, P. M., and Cerveñansky, C. (2005) Conserved autophosphorylation pattern in activation loops and juxtamembrane regions of *Mycobacterium tuberculosis* Ser/Thr protein kinases. *Biochem. Biophys. Res. Commun.* **333,** 858–867
57. Molle, V., Zanella-Cleon, I., Robin, J. P., Mallejac, S., Cozzone, A. J., and Becchi, M. (2006) Characterization of the phosphorylation sites of *Mycobacterium tuberculosis* serine/threonine protein kinases, PknA, PknD, PknE, and PknH by mass spectrometry. *Proteomics* **6,** 3754–3766
58. Arora, G., Sajid, A., Gupta, M., Bhaduri, A., Kumar, P., Basu-Modak, S., and Singh, Y. (2010) Understanding the role of PknJ in *Mycobacterium tuberculosis*: biochemical characterization and identification of novel substrate pyruvate kinase A. *PLoS One* **5,** e10772
59. Scherr, N., Müller, P., Perisa, D., Combaluzier, B., Jenö, P., and Pieters, J. (2009) Survival of pathogenic mycobacteria in macrophages is mediated through autophosphorylation of protein kinase G. *J. Bacteriol.* **191,** 4546–4554
60. Ortega, C., Liao, R., Anderson, L. N., Rustad, T., Ollodart, A. R., Wright, A. T., Sherman, D. R., and Grundner, C. (2014) *Mycobacterium tuberculosis* Ser/Thr protein kinase B mediates an oxygen-dependent replication switch. *PLoS Biol.* **12,** e1001746
61. Fleurie, A., Manuse, S., Zhao, C., Campo, N., Cluzel, C., Lavergne, J. P., Freton, C., Combet, C., Guiral, S., Soufi, B., Macek, B., Kuru, E., VanNieuwenhze, M. S., Brun, Y. V., Di Guilmi, A. M., Claverys, J. P., Galinier, A., and Grangeasse, C. (2014) Interplay of the serine/threonine-kinase StkP and the paralogs DivIVA and GpsB in pneumococcal cell elongation and division. *PLoS Genet.* **10,** e1004275

Protein Kinase A (PknA) of *Mycobacterium tuberculosis* Is Independently Activated and Is Critical for Growth *in Vitro* and Survival of the Pathogen in the Host

Sathya Narayanan Nagarajan, Sandeep Upadhyay, Yogesh Chawla, Shazia Khan, Saba Naz, Jayashree Subramanian, Sheetal Gandotra and Vinay Kumar Nandicoori

J. Biol. Chem. 2015, 290:9626-9645.
doi: 10.1074/jbc.M114.611822 originally published online February 20, 2015
